Applied Mathematical Modelling 75 (2019) 349–370

Contents lists available at ScienceDirect

Applied Mathematical Modelling

journal homepage: www.elsevier.com/locate/apm

Efficient strategy for reliability-based optimization design of multidisciplinary coupled system with interval parameters

Ruixing Wang[b,c], Yan Luo[a,*]

[a] School of Mechanical and Electrical Engineering, Beijing University of Chemical Technology, Beijing 100029, China
[b] Key Laboratory for Mechanics in Fluid-Solid Coupling Systems, Institute of Mechanics, Chinese Academy of Sciences, Beijing 100190, China
[c] School of Engineering Sciences, University of Chinese Academy of Sciences, Beijing 100049, China

ARTICLE INFO

Article history:
Received 13 December 2018
Revised 14 May 2019
Accepted 21 May 2019
Available online 29 May 2019

Keywords:
Multidisciplinary design optimization
Non-probabilistic reliability
Uncertainty propagation analysis
Gradient information
Interval reliability displacement

ABSTRACT

Non-probabilistic reliability based multidisciplinary design optimization has been widely acknowledged as an advanced methodology for complex system design when the data is insufficient. In this work, the uncertainty propagation analysis method in multidisciplinary system based on subinterval theory is firstly studied to obtain the uncertain responses. Then, based on the non-probabilistic set theory, the interval reliability based multidisciplinary design optimization model is established. Considering that the gradient information of interval reliability cannot be acquired in the whole design domain, which causes convergence difficulties and prohibitive computation, an interval reliability displacement based multidisciplinary design optimization method is proposed to address the issue. In the proposed method, the interval reliability displacement is introduced to measure the degree of interval reliability. By doing so, not only the connotation of the interval reliability is guaranteed, but more importantly, the partial gradient region for interval reliability is equivalently converted into full gradient region for reliability displacement. Consequently, the gradient information can be acquired under any circumstances and thus the convergence process is highly accelerated by utilizing the gradient optimization algorithms.

1. Introduction

The field of multidisciplinary design optimization (MDO) has emerged as developed approaches for optimizing the design of large coupled system [1]. By solving the MDO problem early in the design process and taking advantage of advanced computational analysis tools, designers can simultaneously improve the design as well as reduce the time and the cost of the design cycle [2]. Furthermore, considering that there inherently exist large quantities and multi-sources of uncertainties in the whole life circle design of large complex system, including structural parameters, material properties, geometric dimensions, boundary conditions, loads and fabrication tolerance, the reliability based MDO (RBMDO), as a new trend of MDO [3,4], has been widely acknowledged as an advanced and potential methodology to obtain the global optimal solution and guarantee the high reliability simultaneously. The successful applications of RBMDO in engineering are frequently reported in recent years [5–11].

* Corresponding author.
E-mail address: luoyan@mail.buct.edu.cn (Y. Luo).

https://doi.org/10.1016/j.apm.2019.05.030
0307-904X/

It is common knowledge that reliability assessment is the foundation of RBMDO. In practice, structural reliability can be divided into probabilistic reliability and non-probabilistic reliability according to the type of uncertainty. Probabilistic reliability based on the classic probability theory has been studied for long, and many reliability analysis methods have been proposed. The reliability index approach [12] describes the probabilistic constraint as a reliability index and many kinds of indexes have been developed, such as the first order reliability analysis method (FORM), the second order reliability analysis method (SORM) and so on. What is more, many works on probabilistic reliability evaluation and design optimization under the frame of MDO have been presented. Huang et al. [13] combined the collaborative optimization framework and the inverse reliability strategy to assess the uncertainty encountered in the multidisciplinary design process, in which FORM and SORM are employed to calculate the probability integration to assess the reliability. McDonald and Mahadevan [14] developed a novel formulation of RBMDO problems with both system and component level reliability constraints.

However, when dealing with probabilistic reliability, a great quantity of information on the uncertainty is required to construct precise distributions of uncertain parameters, which, unfortunately, is not always available or sometimes very expensive to obtain, especially for complex systems. Therefore, in order to tackle with the reliability problem in uncertain system with few data and poor information, Ben-Haim and Elishakoff [15–18] first proposed the concept of "non-probabilistic reliability" in early 1990s. Ever since, the non-probabilistic reliability theory has been intensely researched by many other researchers and got extensive application in both theoretic research and actual engineering [19–24].

According to the state of the art of the non-probabilistic reliability, two categories of non-probabilistic reliability indexes have been developed. On the one hand, Guo [25], Guo and Lu [26] and Kang et al. [27] measured the non-probabilistic reliability by the minimum distance from the origin to the failure surface, which was inspired by FORM in probability theory. On the other hand, Jiang et al. [28] developed an interval satisfaction degree index to quantitatively characterize the possibility that one interval is smaller than another based on an order-relation of interval numbers [29]. Moreover, Wang et al. [30] extended this concept into multi-dimension situation and then established a general measurement of structural non-probabilistic reliability on the basis of the volume ratio principle and interval interference model. Considering that this kind of reliability index provides a definite assessment for the structural safety with non-probabilistic interval parameters, it has been widely introduced and applied in many research fields with non-probabilistic parameters in recent years, such as the non-probabilistic reliability-based topology optimization [31], non-probabilistic time-dependent reliability assessment [32], non-probabilistic stability reliability measure for vibration control system [33], and so on.

Nevertheless, as stated in [34], for the non-probabilistic reliability based design optimization (NRBDO) issue, non-gradient regions always exist for this interval reliability index. Under this circumstance, the traditional gradient-based optimization algorithms are no longer suitable because the lack of gradient information would easily lead to the local optimal solution. Thus, the global optimization algorithms are always adopted to deal with NRBDO problems in existing literatures [28,35–37], however, the computation amount will dramatically increase. More than that, when the global optimization algorithm is integrated into the non-probabilistic reliability based MDO (NRBMDO) cases, the computation would further increase and become unaffordable when the complex systems are involved. All in all, the main obstacles when tackling with the NRBDO problems under this non-probabilistic reliability index can be summarized as: (1) The existing non-gradient regions will result in convergence difficulties when the gradient-based optimization algorithms are utilized and (2) Huge amount of computation will be caused when the global optimization algorithms are adopted.

Moreover, the non-probabilistic model has only been primitively applied to deal with MDO problems involving interval parameters according to the research state of NRBMDO. Li et al. [37] investigated an uncertain multi-objective MDO using interval convex models. Wang et al. [34] attempted to solve the NRBMDO problems by conducting the interval uncertainty analysis, the reliability analysis and MDO in a sequential manner. However, the first-order approximation is used in the deterministic transformation, which could lead to non-convergence for the highly non-linear problem. All in all, compared with the probabilistic reliability based MDO problems, studies on NRBMDO are still not sufficient at present.

Considering this situation, in this work, an efficient strategy is established to improve the efficiency of the NRBMDO issues. In this method, the non-probabilistic reliability is equivalently converted into the dynamic perpendicular displacement from the actual limit-state plane to the referential limit-state plane. Therefore, the partial gradient region for the reliability is equivalently transformed into full gradient region for reliability displacement and thus the convergence process can be greatly accelerated by utilizing the gradient based optimization technique.

The rest of the paper is organized as follows. In Section 2, the subinterval theory based uncertainty analysis method in multidisciplinary coupled system is researched. In Section 3, the reliability analysis based on the area ratio algorithm in multidisciplinary system is elaborated. In Section 4, the non-probabilistic reliability displacement based MDO is expounded, followed by the explanation of the computation procedure. In Section 5, several cases are conducted to demonstrate the efficiency of the proposed methods. Finally, some conclusions are given in Section 6.

2. Uncertainty propagation analysis in multidisciplinary system

2.1. Description of multidisciplinary system with interval parameters

For the sake of simplicity but without losing generality, Fig. 1 illustrates the interrelation in a typical three-discipline coupled system, in which each small block stands for a discipline analysis.

Additionally, the basic concepts and notations utilized in this paper are explained as follows:

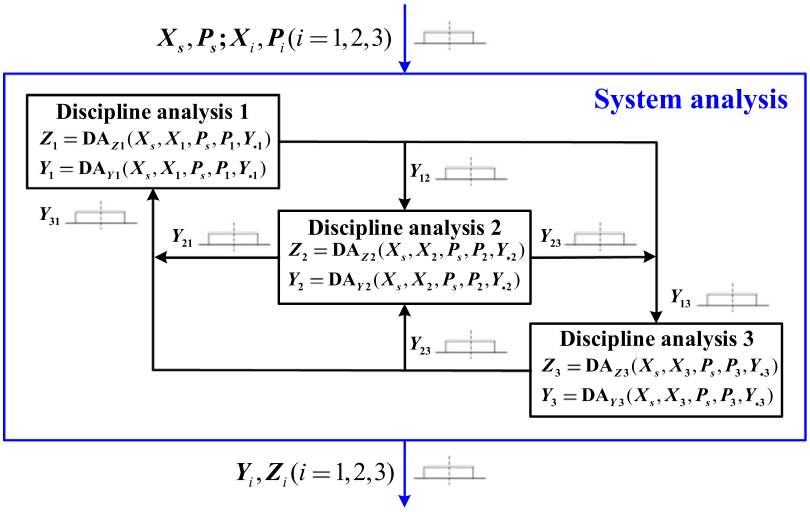

Fig. 1. Concept of a three-discipline coupled system with interval uncertainties.

(1) *Design variables* $\{\boldsymbol{X_s}, \boldsymbol{X_i}\}$: Design variables can be divided into system design variables $\boldsymbol{X_s}$ that involved in more than one discipline and the discipline design variables $\boldsymbol{X_i}$ that only involved in discipline i, $i = 1, \ldots, N$ (N denotes the number of the disciplines). Without loss of generality, the design variables are also assumed to be uncertain.
(2) *Uncertain parameters* $\{\boldsymbol{P_s}, \boldsymbol{P_i}\}$: Just like design variables, uncertain parameters which describes the system attribute can be classified into two types, that is, uncertain system parameters $\boldsymbol{P_s}$ and uncertain discipline parameters $\boldsymbol{P_i}$.

Note that both of the design variables and the uncertain parameters are considered as uncertainties in this paper. In order to express more clearly in the following text, all the involved uncertainties are further divided into two types, namely, system uncertainties $\boldsymbol{U_s}$ and disciplinary uncertainties $\boldsymbol{U_{d\_i}}$ $(i = 1, \ldots, N)$. The expressions of $\boldsymbol{U_s}$ and $\boldsymbol{U_{d\_i}}$ are formulated by

$$\boldsymbol{U}_s = \boldsymbol{X}_s \cup \boldsymbol{P}_s, \qquad \boldsymbol{U}_{d\_i} = \boldsymbol{X}_i \cup \boldsymbol{P}_i \quad (i = 1, \ldots, N) \tag{1}$$

(3) *Linking variables* $\boldsymbol{Y}_{ij} (i \neq j)$: Linking variables represent the variables that acts as the outputs from discipline i and simultaneously the inputs to discipline j.
(4) *System outputs* $\boldsymbol{Z}_i$: System outputs represent the variables that act as the outputs from discipline i, however, not the inputs to any other discipline.
(5) *Discipline analysis DA:* Discipline analysis represents the process that calculates $\boldsymbol{Y}_{ij} (i \neq j)$ and $\boldsymbol{Z}_i$, and the calculation model can be expressed as

$$\begin{aligned} \boldsymbol{Y}_i &= \mathbf{DA}_{Yi}(\boldsymbol{X_s}, \boldsymbol{X}_i, \boldsymbol{P_s}, \boldsymbol{P}_i, \boldsymbol{Y}_{\bullet i}) \\ \boldsymbol{Z}_i &= \mathbf{DA}_{Zi}(\boldsymbol{X_s}, \boldsymbol{X}_i, \boldsymbol{P_s}, \boldsymbol{P}_i, \boldsymbol{Y}_{\bullet i}) \end{aligned} \tag{2}$$

where $\boldsymbol{Y}_i = \{\boldsymbol{Y}_{ij} | j = 1, \ldots, N; j \neq i\}$ denotes the set of linking variables which are the outputs from discipline i and meanwhile the inputs to the other disciplines; $\boldsymbol{Y}_{\bullet i} = \{\boldsymbol{Y}_{1,i}, \ldots, \boldsymbol{Y}_{i-1,i}, \boldsymbol{Y}_{i+1,i}, \ldots, \boldsymbol{Y}_{N,i}\}$ denotes the set of linking variables which are the outputs from all disciplines except discipline i and meanwhile the inputs to discipline i; $\mathbf{DA}_{Yi}$ and $\mathbf{DA}_{Zi}$, respectively, stands for the analysis model for $\boldsymbol{Y}_i$ and $\boldsymbol{Z}_i$.

2.2. Uncertainty propagation analysis based on subinterval theory in multidisciplinary system

The first order interval Taylor expansion algorithm is adopted as the most common way to obtain the interval responses of the multidisciplinary system [38]. However, the method is only accurate for linear system, and the accuracy is supposed to be acceptable when the ranges of the interval parameters are small enough. Actually, for many cases, especially engineering problems, the ranges of the uncertain parameters become so large that the error caused by the first order approximation is unacceptable. In order to address this problem, the subinterval theory is introduced according to [39] and a modified first order interval Taylor expansion method based on global sensitivity equation and subinterval theory is further put forward in this paper.

For convenience, the linking variables $\boldsymbol{Y}_i$ is calculated in the following formulations and for the case of system outputs $\boldsymbol{Z}_i$, the same calculation process can be applied.

Firstly, the system uncertainties $\boldsymbol{U_s}$ and disciplinary uncertainties $\boldsymbol{U}_{d\_i}$ $(i = 1, \ldots, N)$ can be described by interval mathematical theory as follows.

$$\begin{cases} (U_s^i)^c = \frac{\overline{U_s^i}+\underline{U_s^i}}{2}, \quad (U_s^i)^r = \frac{\overline{U_s^i}-\underline{U_s^i}}{2}, \quad i = 1, 2, \ldots, m, \\ (U_{d\_i}^j)^c = \frac{\overline{U_{d\_i}^j}+\underline{U_{d\_i}^j}}{2}, \quad (U_{d\_i}^j)^r = \frac{\overline{U_{d\_i}^j}-\underline{U_{d\_i}^j}}{2}, \quad i = 1, 2, \ldots, N;\ j = 1, 2, \ldots, n_i. \end{cases} \tag{3}$$

where $(U_s^i)^c$ and $(U_{d\_i}^j)^c$ are the median values of U_s^i and $U_{d\_i}^j$; $(U_s^i)^r$ and $(U_{d\_i}^j)^r$ are the interval radius values; $\underline{U_s^i}$ and $\underline{U_{d\_i}^j}$ are the lower bounds; $\overline{U_s^i}$ and $\overline{U_{d\_i}^j}$ are the upper bounds; the number of the elements in $\boldsymbol{U_s}$ is m; the number of elements in $\boldsymbol{U_{d\_i}}$ is n_i. Note that, in this paper, the superscript "r" and "c", respectively, mean the radius and median value; the overline "$\overline{\ }$" and the underline "$\underline{\ }$", respectively, stand for the upper and lower bound.

Secondly, based on the subinterval theory, the large interval uncertainties can be divided into a certain number of small subintervals [40]:

$$(U_s^j)_i = \left[\frac{\underline{U_s^j} + 2(i-1)(U_s^j)^r}{s_j}, \frac{\underline{U_s^j} + 2i(U_s^j)^r}{s_j} \right], \quad i = 1, 2, \ldots, s_j;\ \ j = 1, 2, \ldots, m. \tag{4}$$

where $(U_s^j)_i$ is the ith subinterval of the jth system uncertainties in $\boldsymbol{U_s}$ and s_j is the number of subinterval for U_s^j.

$$(U_{d\_i}^k)_j = \left[\frac{\underline{U_{d\_i}^k} + 2(j-1)(U_{d\_i}^k)^r}{t_{k\_i}}, \frac{\underline{U_{d\_i}^k} + 2j(U_{d\_i}^k)^r}{t_{k\_i}} \right], \quad i = 1, 2, \ldots, N;\ \ j = 1, 2, \ldots, t_{k\_i};\ \ k = 1, 2, \ldots, n_i. \tag{5}$$

where $(U_{d\_i}^k)_j$ is the jth subinterval of the kth uncertainties of the ith discipline and t_{k_i} is the number of subinterval for $U_{d\_i}^k$.

It should be noted here that for the different interval parameters, different number of the subinterval can be applied according to the uncertain level by the guideline provided in [39].

Thirdly, by taking out one subinterval from each interval parameter, w combinations can be generated. And w can be expressed as

$$w = \prod_{i=1}^{m} s_i \times \prod_{i=1}^{N} \prod_{k=1}^{n_i} t_{k\_i} \tag{6}$$

Fourthly, combining the subinterval theory and SIUAM method in [38], the median values of the uncertain multidisciplinary responses for each subinterval combinations can be calculated by one time of multidisciplinary analysis as follows:

$$\begin{aligned} &\boldsymbol{Y}^c_{i\_g_1g_2\ldots g_m h_1^1 h_1^2 \ldots g_{n_N}^N}\left(\alpha_{g_1g_2\ldots g_m}, \beta_{h_1^1 h_1^2 \ldots g_{n_N}^N}\right) = \mathbf{DA}_{\boldsymbol{Y}i}\left(\alpha_{g_1g_2\ldots g_m}, \beta_{h_1^1 h_1^2 \ldots g_{n_N}^N}\right) \\ &g_i = 1, 2, \ldots, s_i, i = 1, 2, \ldots, m; \quad h_k^j = 1, 2, \ldots, t_{j\_k}, k = 1, 2, \ldots, N, j = 1, 2, \ldots, n_N. \end{aligned} \tag{7}$$

where $\alpha_{g_1g_2\ldots g_m}$ is the subinterval vector consisting of the g_ith subinterval of the ith system uncertainty, where $i = 1, 2, \ldots, m$; $\beta_{h_1^1 h_1^2 \ldots g_{n_N}^N}$ is the subinterval vector consisting of the h_k^jth subinterval of the jth uncertainty of the kth discipline, where $j = 1, 2, \ldots, n_N$ and $k = 1, 2, \ldots, N$; $\boldsymbol{Y}^c_{i\_g_1g_2\ldots g_m h_1^1 h_1^2 \ldots g_{n_N}^N}$ is the median values with respect to $\alpha_{g_1g_2\cdots g_m}$ and $\beta_{h_1^1 h_1^2 \cdots g_{n_N}^N}$

And then, the radii of $\boldsymbol{Y}_i$ can be obtained by

$$\boldsymbol{Y}^r_{i\_g_1g_2\cdots g_m h_1^1 h_1^2 \cdots g_{n_N}^N}(\alpha_{g_1g_2\cdots g_m}, \beta_{h_1^1 h_1^2 \ldots g_{n_N}^N}) = (\mathbf{A}^{-1}\mathbf{B}) \times \boldsymbol{U_s^r}(\alpha_{g_1g_2\ldots g_m}) + (\mathbf{A}^{-1}\mathbf{C}) \times \boldsymbol{U_{d\_i}^r}(\beta_{h_1^1 h_1^2 \ldots g_{n_N}^N}) \tag{8}$$

where

$$\mathbf{A} = \begin{bmatrix} \mathbf{I_1} & -\left|\frac{\partial \mathbf{DA}_{\boldsymbol{Y}1}}{\partial \boldsymbol{Y}_{21}}\right| & \cdots & -\left|\frac{\partial \mathbf{DA}_{\boldsymbol{Y}1}}{\partial \boldsymbol{Y}_{n1}}\right| \\ -\left|\frac{\partial \mathbf{DA}_{\boldsymbol{Y}2}}{\partial \boldsymbol{Y}_{12}}\right| & \mathbf{I_2} & \cdots & -\left|\frac{\partial \mathbf{DA}_{\boldsymbol{Y}2}}{\partial \boldsymbol{Y}_{n2}}\right| \\ \vdots & \vdots & \ddots & \vdots \\ -\left|\frac{\partial \mathbf{DA}_{\boldsymbol{Y}n}}{\partial \boldsymbol{Y}_{1n}}\right| & -\left|\frac{\partial \mathbf{DA}_{\boldsymbol{Y}n}}{\partial \boldsymbol{Y}_{2n}}\right| & \cdots & \mathbf{I}_n \end{bmatrix}, \quad \mathbf{B} = \begin{bmatrix} \left|\frac{\partial \mathbf{DA}_{\boldsymbol{Y}1}}{\partial \boldsymbol{U}_s}\right| \\ \left|\frac{\partial \mathbf{DA}_{\boldsymbol{Y}2}}{\partial \boldsymbol{U}_s}\right| \\ \vdots \\ \left|\frac{\partial \mathbf{DA}_{\boldsymbol{Y}n}}{\partial \boldsymbol{U}_s}\right| \end{bmatrix}, \quad \mathbf{C} = diag\begin{bmatrix} \left|\frac{\partial \mathbf{DA}_{\boldsymbol{Y}1}}{\partial \boldsymbol{U}_{d\_i}}\right| \\ \left|\frac{\partial \mathbf{DA}_{\boldsymbol{Y}2}}{\partial \boldsymbol{U}_{d\_i}}\right| \\ \vdots \\ \left|\frac{\partial \mathbf{DA}_{\boldsymbol{Y}n}}{\partial \boldsymbol{U}_{d\_i}}\right| \end{bmatrix}$$

where "*diag*" means the diagonal matrix.

Consequently, the responses bounds for each subinterval combinations can be expressed as

$$\begin{cases} \overline{\boldsymbol{Y}_{i\_g_1g_2\ldots g_m h_1^1 h_1^2 \ldots g_{n_N}^N}} = \boldsymbol{Y}^c_{i\_g_1g_2\ldots g_m h_1^1 h_1^2 \ldots g_{n_N}^N} + \boldsymbol{Y}^r_{i\_g_1g_2\ldots g_m h_1^1 h_1^2 \ldots g_{n_N}^N} \\ \underline{\boldsymbol{Y}_{i\_g_1g_2\ldots g_m h_1^1 h_1^2 \ldots g_{n_N}^N}} = \boldsymbol{Y}^c_{i\_g_1g_2\cdots g_m h_1^1 h_1^2 \ldots g_{n_N}^N} - \boldsymbol{Y}^r_{i\_g_1g_2\cdots g_m h_1^1 h_1^2 \ldots g_{n_N}^N} \end{cases} \tag{9}$$

Obviously, the interval responses with respect to the subintervals are connected one by one. Therefore, the whole interval responses with regards to the original interval vector can be assembled by interval union operation as follows:

$$\boldsymbol{Y}_i = \bigcup_{\substack{g_i=1,2,\cdots,s_i \\ i=1,2,\cdots,m \\ h_k^j=1,2,\cdots,t_{j\_k} \\ k=1,2,\cdots,N \\ j=1,2,\cdots,n_N}} \boldsymbol{Y}_{i\_g_1g_2\cdots g_m h_1^1 h_1^2 \cdots g_{n_N}^N} = \left[\min_{\substack{g_i=1,2,\cdots,s_i \\ i=1,2,\cdots,m \\ h_k^j=1,2,\cdots,t_{j\_k} \\ k=1,2,\cdots,N \\ j=1,2,\cdots,n_N}} \underline{\boldsymbol{Y}_{i\_g_1g_2\cdots g_m h_1^1 h_1^2 \cdots g_{n_N}^N}}, \max_{\substack{g_i=1,2,\cdots,s_i \\ i=1,2,\cdots,m \\ h_k^j=1,2,\cdots,t_{j\_k} \\ k=1,2,\cdots,N \\ j=1,2,\cdots,n_N}} \overline{\boldsymbol{Y}_{i\_g_1g_2\cdots g_m h_1^1 h_1^2 \cdots g_{n_N}^N}} \right] \tag{10}$$

To sum up, by dividing the original uncertain parameters in multidisciplinary system into enough small subintervals, the interval response for each subinterval combination can be guaranteed to be enough precise. Based on this, the accuracy of the whole responses of the multidisciplinary system can be also ensured through the set operation.

However, it should be noted that as the first order interval Taylor expansion method is only accurate for the linear system, it is necessary to divide the original large intervals into a large number of enough small subintervals to guarantee the precise in complex multidisciplinary system. In the case, when there are too many uncertain parameters involved, the subinterval theory based uncertainty analysis method proposed in the paper will suffer unbearable computation on account the fact that too many subinterval combinations are needed. In order to overcome these difficulties to some extent, the following strategies can be implemented:

(1) To reduce the computation caused by the large amount of subinterval combinations, the efficient subinterval decomposition algorithms [41] can be utilized. Therefore, the interval responses of the multidisciplinary system are approximately calculated by only a few subinterval combinational analyses instead of all possible combinations of subintervals.
(2) Some alternative methods are needed to guarantee the efficiency and accuracy. Actually, as stated in [34,38], several uncertainty based multidisciplinary analysis methods under non-probabilistic theory have been proposed, including the iteration algorithm based approach, the direct optimization approach, the interval vertex method and the hybrid concurrent approach. In a manner of speaking, the subinterval theory based uncertainty analysis method in multidisciplinary system proposed in this paper is a complement to the UMDA methodology. In actual engineering projects, we are supposed to choose which method to be utilized in light of actual situations.

3. Interval reliability index based multidisciplinary design optimization

3.1. Interval reliability analysis in multidisciplinary system

As explained in [30], the non-probabilistic interval interference model can provide a reasonable assessment for the state of different interval responses. Therefore, in this work, this model is extended to the multidisciplinary system to appropriately evaluate the system safety. And the limit-state function vector of the multidisciplinary system can be preliminarily expressed as

$$\boldsymbol{G}_i = \boldsymbol{R}_i^{\text{actual}} - \boldsymbol{R}_i^{\text{allowable}} \qquad (i = 1, 2, \ldots, N) \tag{11}$$

where $\boldsymbol{G}_i$ represents the limit-state function vector of discipline i; $\boldsymbol{R}_i^{\text{actual}}$ denotes the actual multidisciplinary response vector of discipline i, which can be acquired by the methods in Section 2; $\boldsymbol{R}_i^{\text{allowable}}$ denotes the allowable multidisciplinary response vector of discipline i, which can be obtained from measurement data, engineering experience, etc.

Furthermore, to facilitate the expression in the follow-up content, the limit-state function vector can be unified for different types of responses as follows.

$$\boldsymbol{M} = \boldsymbol{T} - \boldsymbol{T}^0 \tag{12}$$

where $\boldsymbol{T}$ equals to either of $\boldsymbol{R}^{\text{actual}}$ and $\boldsymbol{R}^{\text{allowable}}$ while $\boldsymbol{T}^0$ equals to the other; $\boldsymbol{M} > \boldsymbol{0}$ indicates the safe state while $\boldsymbol{M} \le \boldsymbol{0}$ indicates dangerous state.

It is widely acknowledged that $\boldsymbol{T}$ and $\boldsymbol{T}^0$ are affected by various uncertainties in actual projects, such as the variability of loads, the dispersion of material properties, the machine tolerance of geometry dimensions, etc. Moreover, the information about uncertain parameters is always poor in the engineering practice. Under this circumstance, the uncertainties are expressed as interval parameters in this paper, and then the element of $\boldsymbol{T}$ and $\boldsymbol{T}^0$ can be described as

$$\begin{cases} T_{i,j} \in \left[\underline{T_{i,j}}, \overline{T_{i,j}}\right] \\ T_{i,j}^0 \in \left[\underline{T_{i,j}^0}, \overline{T_{i,j}^0}\right] \end{cases} \qquad i = 1, 2, \ldots, N;\ j = 1, 2, \ldots, m_i; \tag{13}$$

where m_i denotes the number of limit-state functions in disciplinary i. Moreover, the total number of the limit-state functions is denoted as N_t, which is equal to $\sum_{i=1}^{n} m_i$.

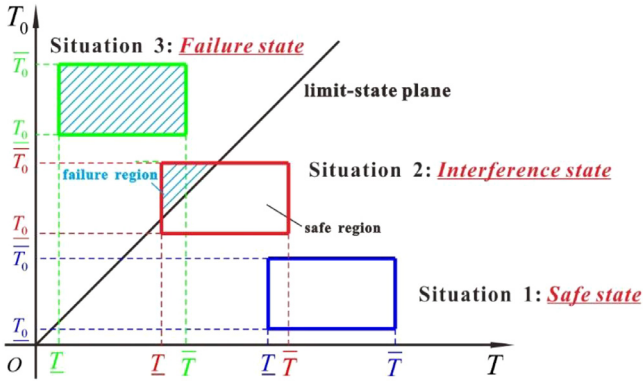

Fig. 2. States of T and T^0 in the two dimensional coordinate system.

For generality and simplification, Eq. (14) is defined as the typical limit-state function

$$M = T - T^0 \tag{14}$$

where $T \in [\underline{T}, \overline{T}], T_0 \in [\underline{T_0}, \overline{T_0}]$.

Based on the interval locations of T and T^0, three situations, namely, the safe state, the interference state and the failure interference, need to be analyzed. As shown in Fig. 2, each of the situations can be illustrated in the two dimensional coordinate system. In order to appropriately evaluate the interval reliability of each situation, the non-probabilistic reliability index that proposed in [30] is introduced and the measure of the structural safety is defined as the ratio of the safe region area to the total area. The expression of the reliability can be expressed by

$$\eta(T > 0) = \eta(T - T_0 > 0) = S_{\text{safe}}/S_{\text{total}} \tag{15}$$

where $\eta(\bullet)$ denotes the possibility, and S stands for the area derived from interval model.

3.2. Formulation of the interval reliability index based MDO optimization model

Considering that the design variables $\boldsymbol{X}_s$ and $\boldsymbol{X}_i$ $(i = 1, \ldots, N)$ as well as the model parameters $\boldsymbol{P}_s$ and $\boldsymbol{P}_i$ $(i = 1, \ldots, N)$ are uncertain in the multidisciplinary system, the general NRBMDO model, that is, the interval reliability index based MDO (IRIB-MDO) model can be mathematically written as follows.

$$\begin{cases} find \quad \boldsymbol{X}^c \\ \min \quad f(\boldsymbol{X}^c) \\ s.t. \quad \boldsymbol{\eta}\{\boldsymbol{M} \geq \boldsymbol{0}\} \geq \boldsymbol{\eta_0} \\ \qquad \boldsymbol{Y}_i = \mathbf{DA}_{Yi}(\boldsymbol{X}, \boldsymbol{Y}_{\bullet i}, \boldsymbol{P}) \\ \qquad \boldsymbol{Z}_i = \mathbf{DA}_{Zi}(\boldsymbol{X}, \boldsymbol{Y}_{\bullet i}, \boldsymbol{P}) \\ \qquad \boldsymbol{X} = (\bigcup_{i=1,\cdots,N} \boldsymbol{X}_i) \cup \boldsymbol{X}_s, \quad \boldsymbol{P} = (\bigcup_{i=1,\cdots,N} \boldsymbol{P}_i) \cup \boldsymbol{P}_s \\ \qquad \boldsymbol{Y}_{\bullet i} \subseteq (\bigcup_{i=1,\cdots,N, j \neq i} \boldsymbol{Y}_j), \quad \boldsymbol{X}^c \in \left[\boldsymbol{X}^L, \boldsymbol{X}^U\right] \end{cases} \tag{16}$$

where $\boldsymbol{X}$ is the design variables set containing both system design variables $\boldsymbol{X}_i$ and discipline design variables $\boldsymbol{X}_s$; $\boldsymbol{X}^c$ represents the median value of $\boldsymbol{X}$, whose feasible design domain is $[\boldsymbol{X}^L, \boldsymbol{X}^U]$; $f(\boldsymbol{X}^c)$ is the objective function to be minimized; $\boldsymbol{\eta_0} = [\eta_0^1, \ldots, \eta_0^{N_t}]$ is the allowable reliability vector, which can be calculated by the non-probabilistic reliability index in Section 3.1. Additionally, the definition of the other parameters can be found in Section 2.

4. Interval reliability displacement based multidisciplinary design optimization

4.1. The statement about the deficiency of IRIB-MDO

The regular strategy based on IRIB-MDO is a direct way to solve NRBMDO problem. It executes interval reliability analysis at every search point and then compares the interval reliability vector with the allowable one to judge if the reliability requirements are satisfied or not. Though the regular solution strategy is understandable, there indeed exist some insufficiencies. For instance, although the interval reliability based on the volume ratio theory possess clearer physical interpretation than any other interval reliability indexes for the interference situation, the gradient information of reliability cannot be gathered in the no interference situation for that the reliability is identically equal to 1 or 0.

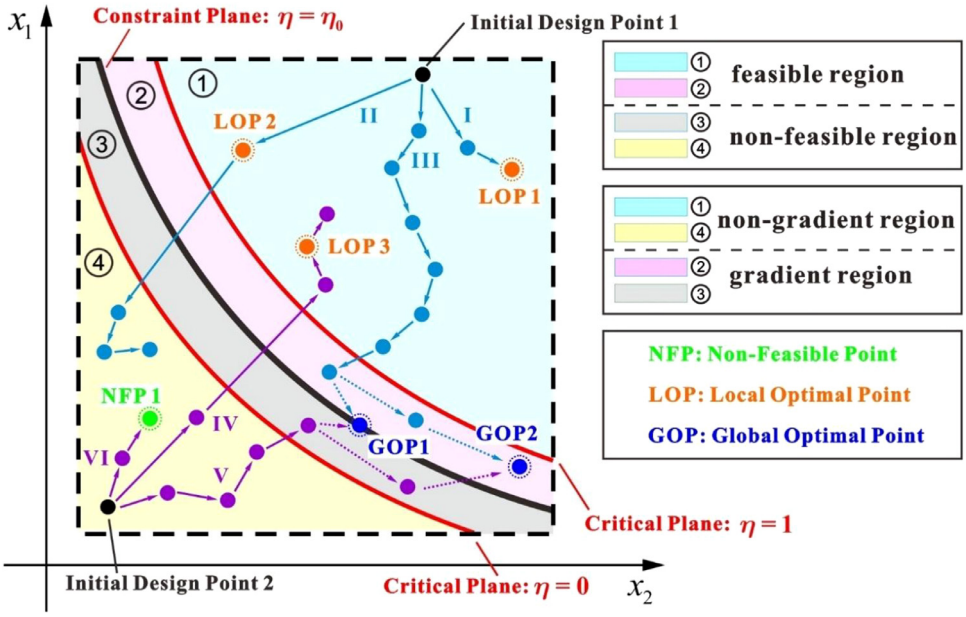

Fig. 3. Six different optimization processes in the IRB-MDO problem.

Consequently, the convergence process may be misguided and delayed when the traditional gradient-based optimization algorithms are utilized to solve the IRB-MDO problem. In order to explain the problem clearly, the following situations are analyzed in detail as illustrated in Fig. 3, which describes the optimization process of a two-variable IRB-MDO problem. Obviously, the whole design space can be divided into four parts by the reliability constraint plane $\eta = \eta_0$, the critical plane $\eta = 0$ and $\eta = 1$. The four regions are denoted as ①, ②, ③, ④ and fall into two categories according to different characteristics. For one thing, ① and ② construct the feasible region while ③, ④ the non-feasible region. For another, ① and ④ construct the non-gradient region while ② and ③ the gradient region. Based on this, the following cases could happen.

When the initial design point is located in the region ① (the feasible and non-gradient region), there exist three possible situations just like the optimization process I, II and III depicted in Fig. 3. All the three processes can be explained as follows:

(1) In the optimization process I, the searching process is "lost" and the solution converges to the local optimal point 1 (LOP 1) in the region ① because the gradient and direction information cannot be acquired.
(2) In the optimization process II, the searching point repeatedly jumps between the region ① (the feasible and non-gradient region) and the region ④ (the non-feasible and non-gradient region), then the searching process is "lost" in the non-gradient region ④ and the solution would converge to the previous optimal design point, namely the LOP 2 in the region ①.
(3) In the optimization process III, after many times of nondirectional search, the searching point finally jumps into the gradient region, and then it will converge to the global optimal points (GOP1 and GOP2) rapidly. However, the optimization process is indeed delayed in process of nondirectional search.

When the initial design point is located in the region ④ (the non-feasible and non-gradient region), there also exist three situations just like the optimization process IV, V and VI delineated in Fig. 3. Similarly, the three processes can be described as

(1) In the optimization process IV, the searching point jumps from the non-feasible region ④ to the feasible region ①. And then it is "lost" in the non-gradient region ① and converges to the LOP 3.
(2) In the optimization process V, just like the process III, though the searching process will finally converge to either GOP1 or GOP2 rapidly, the convergence will be delayed for the nondirectional search into the gradient region.
(3) In the optimization process VI, the searching process is "lost" in the non-gradient region ④ and only the non-feasible design points are detected. Therefore, the feasible design point cannot be acquired in this situation, let alone the global optimal point.

All in all, for the IRB-MDO issues, due to the lack of gradient information of interval reliability, the situations where the optimization processes are misguided do exist. The facts will be further demonstrated in the numerical examples in Section 5. Moreover, it should be noted that the risk of falling into the local optimal point and non-feasible point will increase as the area rate of the gradient region decreases. In this case, the global optimization algorithm will be an alternate but with a sharp reduction of computational efficiency. Consequently, in this paper, we intend to develop a novel strategy in

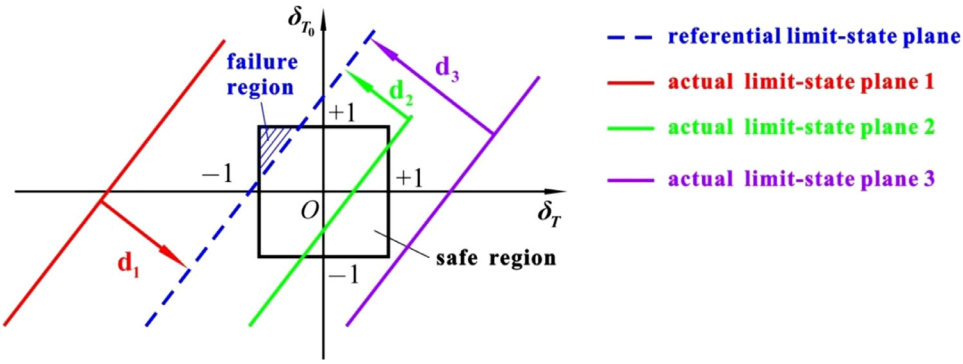

Fig. 4. Displacement from the actual limit-state plane to the referential limit-state plane.

which the gradient-based optimization algorithms can be applied to deal with the IRB-MDO issue to increase the efficiency in the premise of accuracy.

4.2. The definition of the interval reliability displacement

In view of the above considerations, some improvements have been achieved in this section to ameliorate the situations. The key issue is to seek an equivalent transformation of the interval reliability, which cannot only maintain the meaning of reliability in Section 3.1, but also gain the gradient information to get the right search direction.

For better understanding and clearer analytic process, the interval model is firstly converted into the normalized space according to the following transformation equation:

$$\begin{cases} \delta_T = (T - T^c)/T^r, \quad \text{where } T^c = (\overline{T} + \underline{T})/2 \text{ and } T^r = (\overline{T} - \underline{T})/2 \\ \delta_{T_0} = (T_0 - T_0^c)/T_0^r, \quad \text{where } T_0^c = (\overline{T_0} + \underline{T_0})/2 \text{ and } T_0^r = (\overline{T_0} - \underline{T_0})/2 \end{cases} \tag{17}$$

where δ_T and δ_{T_0} are the normalized interval variables.

Substituting Eq. (17) into Eqs. (14) and (15), the limit-state function and reliability index function can be obtained as

$$M(\delta_T, \delta_{T_0}) = T^r \delta_T - T_0^r \delta_{T_0} + (T^c - T_0^c) \tag{18}$$

$$\eta(M(\delta_T, \delta_{T_0}) > 0) = \eta(T^r \delta_T - T_0^r \delta_{T_0} + (T^c - T_0^c) > 0) = \frac{S_{\text{safe}}}{S_{\text{total}}} \tag{19}$$

Then, in order to expound this issue more clearly, as illustrated in Fig. 4, we define the following two notions:

(1) **Referential limit-state plane:** a plane which is parallel to the actual limit-state plane and the interval reliability is the allowable reliability η_0.
(2) **Interval reliability displacement:** the dynamic perpendicular displacement that the actual limit-state plane shifts to the referential limit-state plane, which is denoted as d. The reliability displacement is positive when the actual limit-state plane shifts in the direction of positive δ_T axis, otherwise, the reliability displacement is negative.

Obviously, when $d \geq 0$, we can draw the conclusion that the structure is safe and the design is conservative, and what is more, the conservative degree of the actual limit-state plane can be also measured by d in no matter the interference situation or the no interference situation. Similarly, when $d < 0$, we will reach the conclusion that the structure is dangerous, the design is radical and the radical degree is also quantified by d.

Therefore, the interval reliability displacement acts as an equivalent transformation of the interval reliability. More importantly, the gradient information of the reliability displacement is acquired all through the optimization process. It should be noted here is that the actual/referential limit-state plane is dynamic in the optimization process. Just as shown in Fig. 5, though the interval reliability corresponding to the referential limit-state plane always equals to the allowable reliability η_0, the slope of the referential limit-plane keeps changing from the iteration step 1 till the iteration step n until the convergence is achieved.

4.3. The analytic solution of the interval reliability displacement

In order to obtain the interval reliability displacement, the expression of the referential limit-state plane needs to be acquired. Considering the normalized actual limit-state function shown in Eq. (18), the referential limit-state plane whose slope is same as the normalized actual limit-state function can be written as

$$T^r \delta_T - T_0^r \delta_{T_0} + D^{\text{referential}} = 0 \tag{20}$$

where $D^{\text{referential}}$ is an undetermined item that needs to be derived.

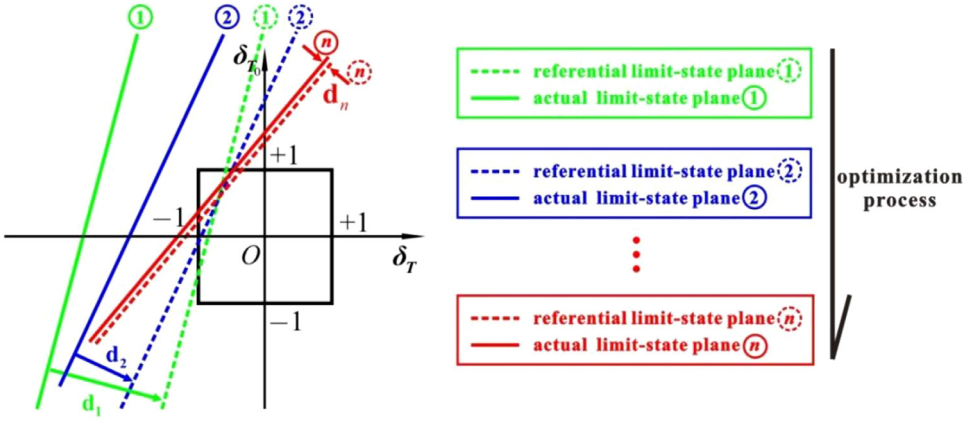

Fig. 5. Dynamic actual/referential limit-state plane during the optimization process.

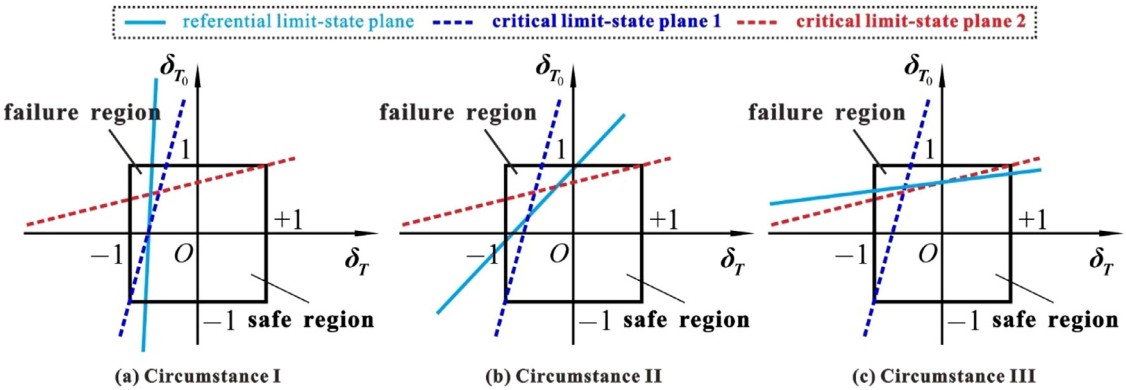

Fig. 6. Illustration of the three circumstances according to the slope value.

Note that the allowable reliability η_0 is always assigned a value close to 1 to ensure safety in practical engineering, thus the referential limit-state plane is located at the upper-left corner of the normalized feasible region. In this case, three circumstances shown in Fig. 6 is analyzed to acquire the solution of $D^{\text{referential}}$ according to the slope value. To identify the three circumstances, two critical limit-state planes that cross the points $(-1, -1)$ and $(1, 1)$ are introduced. And based on the area-ratio principle, the critical slope values can be calculated by:

$$\begin{cases} \text{critical limit} - \text{state plane 1}: \quad \eta_0 = 1 - \frac{S_{faliure}}{S_{total}} = 1 - \frac{\frac{1}{2} \times \frac{2}{Slope_1} \times 2}{4} \quad \Rightarrow Slope_1 = \frac{1}{2(1-\eta_0)} \\ \text{critical limit} - \text{state plane 2}: \quad \eta_0 = 1 - \frac{S_{faliure}}{S_{total}} = 1 - \frac{\frac{1}{2} \times 2Slope_2 \times 2}{4} \quad \Rightarrow Slope_2 = 2(1-\eta_0) \end{cases} \tag{21}$$

where $Slope_1$ and $Slope_2$ are the slope of the critical limit-state plane 1 and 2, respectively.

Then, $D^{\text{referential}}$ is supposed to be deduced according to the following three circumstances.

(1) Circumstance I: $T_0^r/T^r \geq slope_1$

As illustrated in Fig. 6(a), the referential limit-state plane intersects with the upper and lower sides of the feasible region, thereby the failure region is constructed by an right-angled trapezoid in this circumstance. The four vertexes coordinates of the right-angled trapezoid can be obtained as $(-1, 1)$, $(-1, -1)$, $((T_0^r - D^{\text{referential}})/T^r, 1)$, $((-T_0^r - D^{\text{referential}})/T^r, -1)$. Considering that, the equation of calculating the reliability can be formulated by

$$\eta_0 = 1 - \frac{S_{\text{failure}}}{S_{\text{total}}} = 1 - \frac{\frac{1}{2} \times 2 \times \left(\frac{T_0^r - D^{\text{referential}}}{T_0^r} + 1 + \frac{-T_0^r - D^{\text{referential}}}{T_0^r} + 1 \right)}{4} \tag{22}$$

Therefore, $D^{\text{referential}}$ can be obtained by solving Eq. (22).

$$D^{\text{referential}} = (2\eta_0 - 1)T^r \tag{23}$$

(2) Circumstance II: $slope_2 < T_0^r/T^r < slope_1$

As illustrated in Fig. 6(b), the referential limit-state plane intersects with the left and upper sides of the feasible region, thereby the failure region is constructed by an right angle triangle in this circumstance. The three vertexes coordinates of

the right angle triangle can be obtained as $(-1, 1)$, $((T_0^r - D^{\text{referential}})/T_0^r, 1)$, $(-1, (-T_0^r + D^{\text{referential}})/T_0^r)$. Considering that, the equation of calculating the reliability can be formulated by

$$\eta_0 = 1 - \frac{S_{\text{failure}}}{S_{\text{total}}} = 1 - \frac{\frac{1}{2} \times \left(\frac{T_0^r - D^{\text{referential}}}{T^r} + 1\right)\left(1 - \frac{-T_0^r + D^{\text{referential}}}{T_0^r}\right)}{4} \tag{24}$$

Therefore, $D^{\text{referential}}$ can be obtained by solving Eq. (24).

$$D^{\text{referential}} = {T_0}^r + T^r - \sqrt{8T^r{T_0}^r(1-\eta_0)} \tag{25}$$

(3) Circumstance III: $T_0^r/T^r \le slope_2$

As illustrated in Fig. 6(c), the referential limit-state plane intersects with the left and right sides of the feasible region, thereby the failure region is constructed by an right-angled trapezoid in this circumstance. The four vertexes coordinates of the right-angled trapezoid can be obtained as $(-1, 1)$, $(1, 1)$, $(1, (T^r + D^{\text{referential}})/T_0^r)$, $(-1, (-T_0^r + D^{\text{referential}})/T_0^r)$. Considering that, the equation of calculating the reliability can be formulated by

$$\eta_0 = 1 - \frac{S_{\text{failure}}}{S_{\text{total}}} = 1 - \frac{\frac{1}{2} \times 2 \times \left(\frac{T_0^r - D^{\text{referential}}}{T_0^r} + 1 + \frac{-T_0^r - D^{\text{referential}}}{T_0^r} + 1\right)}{4} \tag{26}$$

Therefore, $D^{\text{referential}}$ can be obtained by solving Eq. (26).

$$D^{\text{referential}} = (2\eta_0 - 1)T_0^r \tag{27}$$

Furthermore, based on the above analysis and the definition proposed in Section 4.2, the interval reliability displacement d can be computed as

$$d = \frac{T^c - {T_0}^c - D^{\text{referential}}}{\sqrt{(T^r)^2 + ({T_0}^r)^2}} \tag{28}$$

Consequently, the expressions of d under different conditions can be summarized as

$$d = \begin{cases} \frac{T^c - {T_0}^c - (2\eta_0 - 1)T^r}{\sqrt{(T^r)^2 + ({T_0}^r)^2}}, & \frac{T_0^r}{T^r} \ge \frac{1}{2(1-\eta_0)} \\ \frac{T^c - {T_0}^c - T^r - {T_0}^r + \sqrt{8T^r{T_0}^r(1-\eta_0)}}{\sqrt{(T^r)^2 + ({T_0}^r)^2}}, & 2(1-\eta_0) < \frac{T_0^r}{T^r} < \frac{1}{2(1-\eta_0)} \\ \frac{T^c - {T_0}^c - (2\eta_0 - 1){T_0}^r}{\sqrt{(T^r)^2 + ({T_0}^r)^2}}, & \frac{T_0^r}{T^r} \le 2(1-\eta_0) \end{cases} \tag{29}$$

Consequently, the new optimization model based on the reliability displacement can be developed from Eq. (16) as

$$\begin{cases} find \quad \boldsymbol{X}^c \\ \min \quad f(\boldsymbol{X}^c) \\ s.t. \quad \boldsymbol{d} \ge \boldsymbol{0} \\ \qquad \boldsymbol{Y}_i = \mathbf{DA}_{Yi}(\boldsymbol{X}, \boldsymbol{Y}_{\bullet i}, \boldsymbol{P}) \\ \qquad \boldsymbol{Z}_i = \mathbf{DA}_{Zi}(\boldsymbol{X}, \boldsymbol{Y}_{\bullet i}, \boldsymbol{P}) \\ \qquad \boldsymbol{X} = (\bigcup_{i=1,\dots,N} \boldsymbol{X}_i) \cup \boldsymbol{X}_s, \quad \boldsymbol{P} = (\bigcup_{i=1,\dots,N} \boldsymbol{P}_i) \cup \boldsymbol{P}_s \\ \qquad \boldsymbol{Y}_{\bullet i} \subseteq (\bigcup_{i=1,\dots,N, j \ne i} \boldsymbol{Y}_j), \quad \boldsymbol{X}^c \in \left[\boldsymbol{X}^L, \boldsymbol{X}^U\right] \end{cases} \tag{30}$$

where $\boldsymbol{d} = [d_1, \dots, d_{N_t}]$ is the interval reliability displacement vector.

On this basis, corresponding to Fig. 3, the searching process of the above optimization model can be illustrated in Fig. 7. Apparently, the whole design space, which is composed by feasible region and non-feasible region, is supposed to be a whole gradient field when the reliability displacement constraint is considered. Based on this, the following processes will happen.

(1) When the initial design point is located in the feasible region, as shown in Fig. 7, just like the optimization process I, the searching process converges to the global optimal point because the gradient and direction information can be easily acquired.
(2) When the initial design point is located in the non-feasible region, just like the optimization process II, the searching process also can converge to the global optimal point because the gradient and direction information can be easily acquired as well.

Therefore, the conclusion can be drawn that, compared with IRIB-MDO, IRDB-MDO has higher efficiency by converting the non-gradient problem into an equivalent gradient issue.

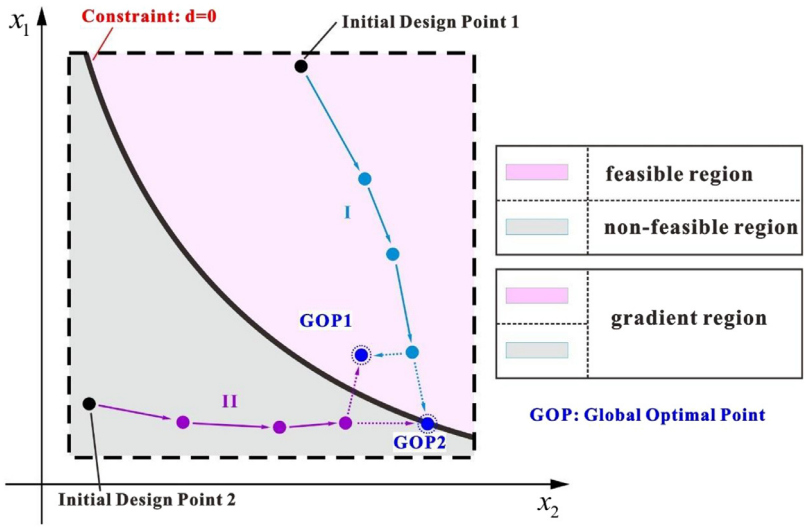

Fig. 7. Two different optimization processes in IRDB-MDO.

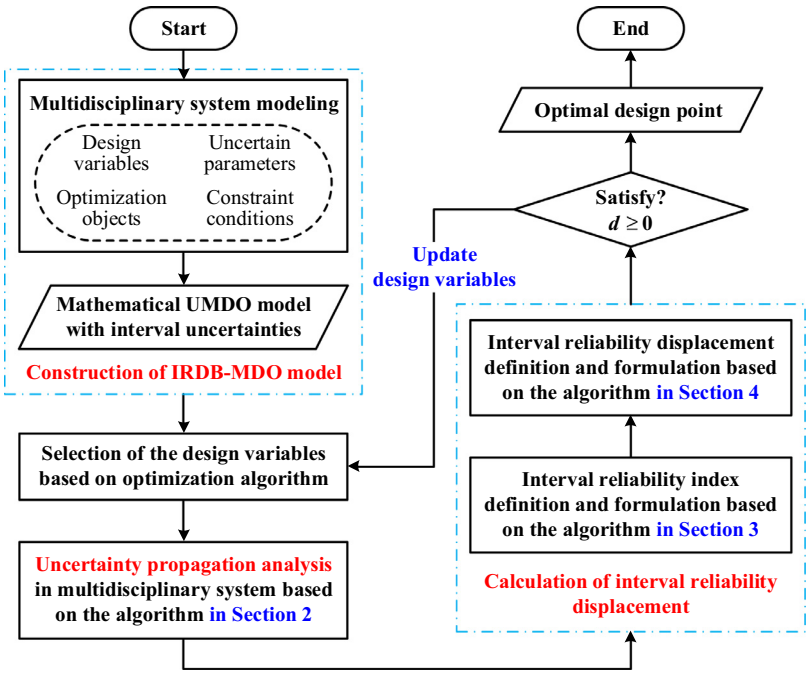

Fig. 8. Computational procedure of IRDB-MDO.

4.4. Computational procedure of IRDB-MDO

In this section, we will emphasize the optimization design process based on the proposed strategy. The flowchart of IRDB-MDO is illustrated in Fig. 8 and the specified computational procedure can be expounded as follows:

(1) Construct the IRDB-MDO model with mathematical description. Model the practical multidisciplinary design problem, including identifying the design variables, system parameters, the constraint conditions, optimization objects, design space. Then, establish the mathematical optimization model of the IRBMDO problem as shown in Eq. (30).
(2) Conduct the uncertainties propagation analysis at the search point. Select the design point based on the optimization algorithm and then analyze the interval bounds of the multidisciplinary responses through the uncertainty analysis method proposed in Section 2.

(3) Analysis the interval reliability displacement. Based on the uncertain responses obtained in (2) and the interval reliability definition proposed in Section 3, the interval reliability displacement analysis can be accomplished through the method proposed in Section 4.
(4) Check the convergence of the optimization process. If reliability requirements are satisfied and the system objects becomes stable, the entire optimization procedure is regarded to be completed. Otherwise, repeat (2) and (3) to continue the uncertainties propagation analysis and interval reliability displacement analysis at the updated search point.
(5) Export the optimal solutions. The optimal design point can be acquired after the optimization process converges.

5. Numerical examples and discussions

5.1. Example 1: mathematical function case

The multidisciplinary system involved in this case consists of two disciplines, which are **discipline 1** and **discipline 2**. X_1, X_2, X_3 are design variables, and all of X_1, X_2, X_3 are the system design variables. $p_s, p_1, p_2, g_1^0, g_2^0$ are uncertain parameters, in which p_s is the uncertain system parameter, p_1 and p_2 are uncertain discipline parameters, g_1^0, g_2^0 are the uncertain parameters in constraint functions. Moreover, the allowable reliability vector is specified to be (0.9, 0.9). Thus, the optimization model can be mathematically expressed in Eq. (31) as

$$\begin{cases} \textbf{find} \quad X_1, X_2, X_3 \\ \textbf{minimize} \quad F = (X_1 + \overline{p}_s)^2 + X_2^2 + X_3^2 \\ \textbf{subject to:} \\ \boxed{\begin{array}{l} \text{discipline 1:} \quad 4y_{12} = 2X_1 + 2p_s - 3X_2 + 2X_3 - 4y_{21} \\ \text{constraint 1:} \quad \begin{cases} g_1 = X_1 + p_s + 2X_2 + 2y_{21} - p_1 + 1 \\ \eta_1(g_1 - g_1^0 \geq 0) \geq 0.9 \end{cases} \end{array}} \\ \boxed{\begin{array}{l} \text{discipline 2:} \quad 4y_{21} = -2X_1 - 2p_s - X_2 + 2X_3 + 4y_{12} \\ \text{constraint 2:} \quad \begin{cases} g_2 = 5X_1 - 5p_s + 3X_3 - 4y_{12} - p_2 + 2 \\ \eta_2(g_2 - g_2^0 \geq 0) \geq 0.9 \end{cases} \end{array}} \\ \boxed{\begin{array}{l} \text{design variables:} \quad \begin{array}{l} 1 \leq X_2, X_3 \leq 5 \\ 0 \leq X_1 \leq 5 \end{array} \end{array}} \\ \boxed{\begin{array}{l} \text{uncertain parameters:} \quad \begin{array}{l} p_s \in [0.90, 1.10]; \quad p_1 \in [4.05, 4.95]; \quad p_2 \in [0.95, 1.05] \\ g_1^0 \in [-0.60, 0]; \quad g_2^0 \in [0, 1.00] \end{array} \end{array}} \end{cases} \tag{31}$$

5.1.1. Optimization based on IRIB-MDO

In this part, IRIB-MDO is tried to solve the optimization design problem. In the first place, one of the most common gradient optimization algorithm, namely, the sequential quadratic programming (SQP) is chosen to work out the problem. Unfortunately, the situations in which either the local optimal solution or the non-feasible solution is obtained often happened for the reason that the search points locate in the non-gradient region where the gradient information of interval reliability is always equivalent to 0 and then the search direction is not clear. Different initial design points are selected and the results can be listed in Table 1.

Under this circumstance, the global optimization algorithms are introduced to tackle the problem. When the global optimization strategy is applied, neither the derivative information nor the gradient information is needed. However, the calculation amount sharply increases.

In this case, the initial design point is set to be $(X_1, X_2, X_3) = (2.5, 3.0, 3.0)$ and the converging process based on global optimization method, i.e., adaptive simulated annealing (ASA) is conducted. The obtained optimal point is $(X_1, X_2, X_3) = (0.531, 1.428, 1.728)$ and the minimum value of objective function is $F = 7.369$. Note that the reliability at the optimal point can be obtained based on the area ratio theory and the reliability vector is $\boldsymbol{\eta} = (\eta_1, \eta_2) = (0.9002, 0.9012)$, which means that the reliability requirements have been satisfied.

5.1.2. Optimization based on IRDB-MDO

IRDB-MDO is used to solve the UMDO problem as well. Similar to the strategy in above section, SQP is firstly used to settle the problem. Due to the proper gradient information of interval reliability displacement which can be captured in any search points, the global optimal solution of the optimization problem is easily obtained and the optimization process

Table 1
The optimum solutions based on SQP and ASA for IRIB-MDO.

	Design variables			Object	Constrain reliability		Total MDA
	X_1	X_2	X_3	F	η_1	η_2	
SQP IP 1[a]	1.2506	2.0005	2.0005	13.0690	1.0	1.0	39
SQP IP 2[b]	No feasible design is found to satisfy all constraints						
SQP IP 3[c]	0.6291	1.4289	1.6287	7.3483	0.9	0.9	41
ASA	0.5309	1.4179	1.7283	7.3694	0.9002	0.9012	20,254

[a] IP 1 = (2.5, 3.0, 3.0), which locates in the feasible and non-gradient region.
[b] IP 2 = (0.0, 1.0, 1.0), which locates in the non-feasible and non-gradient region.
[c] IP 3 = (1.0, 1.5, 1.5), which locates in the gradient region.

Table 2
The optimum solutions based on gradient optimization algorithms for IRDB-MDO.

	Design variables			Object	Constraint reliability		Total MDA
	X_1	X_2	X_3	F	η_1	η_2	
SQP IP 1[a]	0.6292	1.4289	1.6286	7.3483	0.9	0.9	17
SQP IP 2[b]	0.6294	1.4289	1.6284	7.3483	0.9	0.9	9
SQP IP 3[c]	0.6292	1.4289	1.6286	7.3483	0.9	0.9	17
MMFD IP 1[a]	0.6289	1.4289	1.6289	7.3483	0.9	0.9	31
MMFD IP 2[b]	0.6305	1.4289	1.6273	7.3483	0.9	0.9	30
MMFD IP 3[c]	0.8289	1.4289	1.4289	7.4283	0.9	0.9	26
LSGRG IP 1[a]	0.6289	1.4289	1.6289	7.3483	0.9	0.9	36
LSGRG IP 2[b]	0.6289	1.4289	1.6289	7.3483	0.9	0.9	26
LSGRG IP 3[c]	0.6289	1.4289	1.6289	7.3483	0.9	0.9	24

[a] IP 1 = (2.5, 3.0, 3.0).
[b] IP 2 = (0.0, 1.0, 1.0).
[c] IP 3 = (1.0, 1.5, 1.5).

Table 3
Optimum solutions of IRIB-MDO and IRDB-MDO.

		Design variables			Object	Constrain reliability		Total MDA
		X_1	X_2	X_3	F	η_1	η_2	
IRIB-MDO	**ASA**	0.5309	1.4179	1.7283	7.3694	0.9002	0.9012	20,254
SLS-NRBMDO	**SQP**[a]	0.6292	1.4289	1.6286	7.3483	0.9	0.9	47
IRDB-MDO	**SQP**[a]	0.6292	1.4289	1.6286	7.3483	0.9	0.9	34

[a] When SQP is utilized, the initial point (1.5, 1.5, 1.0) is selected.

converges quickly. Corresponding to Section 5.1.1, different initial points are selected to verify the effectiveness of the proposed IRDB-MDO. Furthermore, several gradient optimization algorithms, namely, SPQ, MMDF (Modified method of feasible directions), LSGRG (Large Scale Generalized Reduced Gradient), are introduced to tackle this issue. All the results are listed in Table 2.

From the results in Table 2, it indicates that the optimum solutions are acquired when any of the initial design points and gradient optimization algorithms is selected for that the gradient information of the interval reliability displacement constraints is available in any circumstances.

5.1.3. Comparison between IRDB-MDO and the existing algorithms

In order to further illuminate the characteristics of the proposed algorithm, the comparisons between IRDB-MDO and the existing algorithms are conducted. Besides IRIB-MDO, the efficient single-loop strategy SLS_NRBMDO in [34] is also considered.

To compare the efficiency of the three algorithms, the converging processes constituted by improved data points and the optimal solutions for both methods are respectively shown in Fig. 9 and Table 3. Obviously, all the three methods can obtain the optimal solution in this example. On the one hand, the number of total multidisciplinary analyses of IRDB-MDO is at the same level with SLS-NRBMDO since gradient optimum algorithms are applied in both strategies; on the other hand, the computational cost of either SLS-NRBMDO or IRDB-MDO is much less than that of IRIB-MDO because global optimum algorithms are utilized. Another thing to note that though the first-order approximation is used in SLS-NRBMDO, it is still suitable for this case while the nonlinear degree of the multidisciplinary system is not high in this example.

Besides, the gradient information for both constraints of IRID-MDO and IRDB-MDO are contrasted in Fig. 10. Based on the figure, it turns out that for the same design domain, in IRID-MDO strategy, most region of the constraints is non-gradient and only a small region of the constraints is gradient. On the other hand, as an improved strategy, in IRDB-MDO, all the region of constraints is gradient, thus the efficient gradient based optimization algorithms can be applied. Furthermore, the

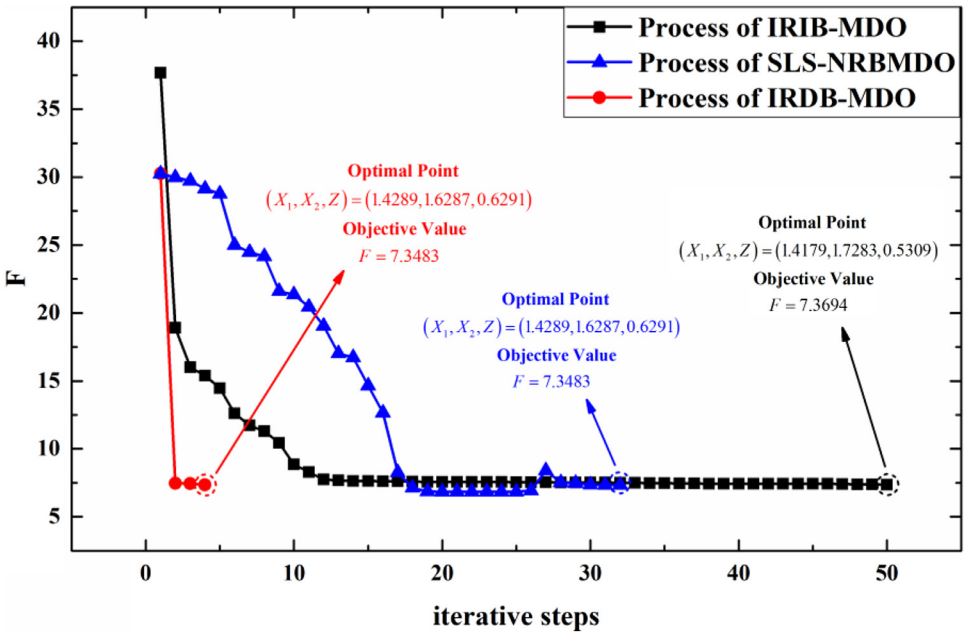

Fig. 9. Converging process of optimization based on IRIB-MDO and IRDB-MDO.

Table 4
Probabilistic and interval reliability analyses in different design schemes.

Design scheme number	IRDB-MDO					MCS	
	Constraint interval reliability		Design scheme			Probabilistic reliability	
	η_1	η_2	X_1	X_2	X_3	η_{1_MSC}	η_{2_MSC}
1	0.80	0.80	0.6101	1.3166	1.6096	0.8390	0.8126
2	0.85	0.85	0.6188	1.3680	1.6183	0.8847	0.8623
3	0.90	0.90	0.6291	1.4289	1.6287	0.9333	0.9121
4	0.95	0.95	0.6427	1.5083	1.6422	0.9735	0.9582

variation ranges of constraints are much larger than that in IRIB-MDO, which only varies between 0 and 1. It means that the gradient feature is more distinct, which makes IRDB-MDO converge much faster than IRID-MDO.

5.1.4. Validation based on MCS

In order to verify the validity of the proposed interval reliability based optimization methods, MSC is applied to demonstrate the optimized design scheme. In this case, the size of the MCS is chosen as 100,000, which is large enough to be considered as the "correct analytic solution" for the purpose of confirmation, and random simulations are picked to follow uniform distributions of the input variables. Taking the optimized design scheme obtained through IRDB-MDO as an example, the reliability obtained by MCS is compared with the constraint reliability, which is assumed to be 0.8, 0.85, 0.9 and 0.95. The probabilistic reliability values of both constraints are listed in Table 4 and the tendency under different constraint interval reliability are illustrated in Fig. 11.

5.2. Example 2: supersonic aircraft conceptual design

The well-studied NASA test suite with regards to the design of a supersonic business jet is adopted in this paper to further illustrate the effectiveness of IRDB-MDO for high dimensional and highly non-linear problems. As illustrated in Fig. 12, the supersonic jet is modeled as a coupled system of structure, aerodynamic, propulsion, and aircraft range. The analysis model involves 8 linking variables, including total aircraft weight W_T, wing twist θ, fuel weight W_F, drag D, drag-to-lift ratio L/D, fuel consumption SFC, engine scale factor ESF, engine weight W_E. The detailed description of the analysis models for all the linking variables and outputs in involving disciplines are presented in [42].

The purpose of the optimization model is to maximize the range R which is computed through the Breguet range equation as follows:

$$R = \frac{M(L/D)661\sqrt{\sigma}}{SFC}\mathrm{In}\left(\frac{W_T}{W_T - W_F}\right) \tag{32}$$

where M is Mach number, σ is temperature ratio.

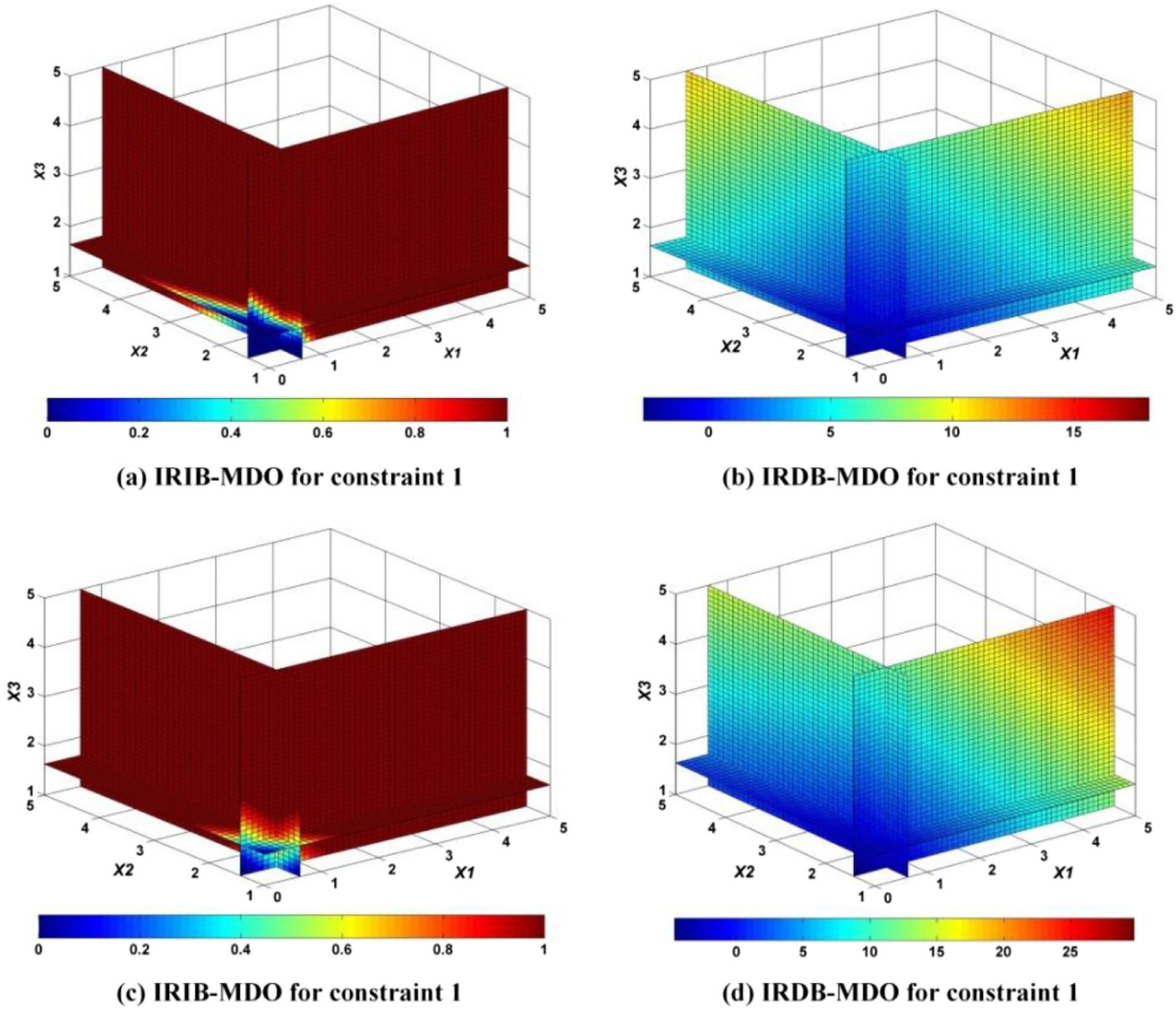

Fig. 10. Illustration of the gradient information for both IRIB-MDO and IRDB-MDO.

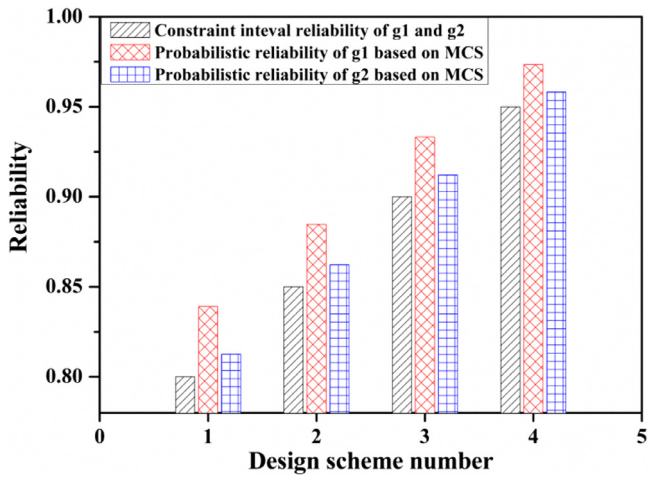

Fig. 11. Comparison between probabilistic reliability and interval reliability for different design scheme.

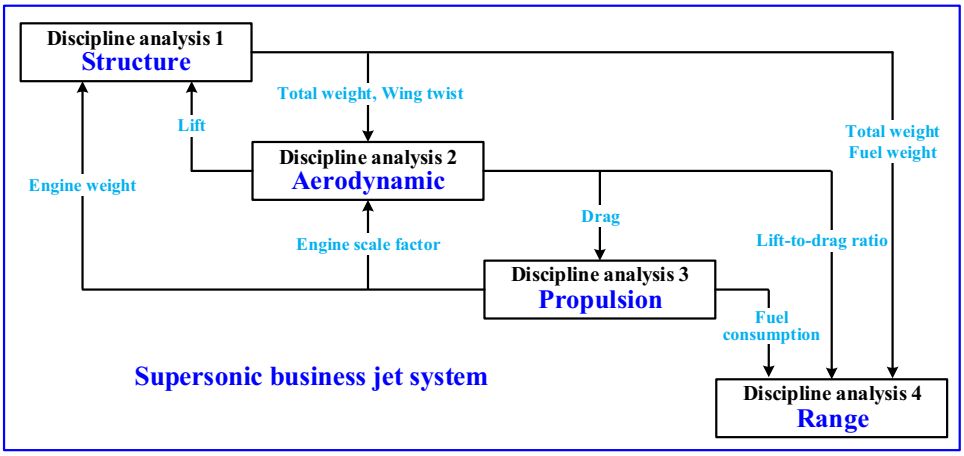

Fig. 12. Illustration of supersonic business jet system consisting of four disciplines.

Table 5
Descriptions of the design variables in case 2.

	Name	Symbol (unit)	Lower bound	Upper bound
1	Wing taper ratio	λ	0.1	0.4
2	Wingbox x-sectional area	χ	0.75	1.25
3	Skin friction coefficient	C_1	0.75	1.25
4	Throttle	T	0.1	1
5	Thickness/chord ratio	t/c	0.01	0.09
6	Altitude	h (ft)	30,000	60,000
7	Mach number	M	1.4	1.8
8	Aspect ratio	AR	2.5	8.5
9	Wing sweep	Λ (°)	40	70
10	Wing surface area	S_{ref} (ft^2)	500	1500

Table 6
Descriptions of the uncertain variables in case 3.

	Mach number M	Altitude h (ft)	Throttle T
Median value	1.4–1.8	30,000–60,000	0.1–1
Deviation	5%	5%	5%

The involving 10 design variables are specifically described in Table 5.

Moreover, in this example, engine scale factor *ESF* and engine temperature *Temp* are chosen as the constraints. The specified expressions can be written as

$$\begin{cases} 0.5 \le ESF = (D/3)/(T * 16168.6) \le 1.5 \\ temp = pf(M, h, T) \le 1.02 \end{cases} \tag{33}$$

where *pf* is the polynomial equation, the definition of that is presented in [42].

Specially, considering that uncertainties are inevitably involved in the process of the supersonic aircraft conceptual design, M, h, T are considered to be uncertainties in the case, and the detailed descriptions of the uncertain variables can be listed in Table 6. Then the constraint equations can be rewritten as follows to consider the interval reliability constraints.

$$\begin{cases} \eta_1(0.5 \le ESF \le 1.5) \ge \eta_0^1 \\ \eta_2(temp \le 1.02) \ge \eta_0^2 \end{cases} \tag{34}$$

where η_1 and η_2 are the actual interval reliability, η_0^1 and η_0^2 are the corresponding allowable reliability. In this case, the values of η_0^1 and η_0^2 is set to be 0.9 and 0.9.

The uncertainty propagation analysis is conducted by the modified first order interval Taylor expansion method proposed in this paper. Note that SLS-NRBMDO is no longer applicable in this example for the high non-linear effect, therefore, only IRDB-MDO and ASA are conducted. Additionally, SQP is utilized in IRDB-MDO while ASA in IRIB-MDO. Then, the optimal design solutions can be listed in Table 7 and the converging processes are illustrated in Fig. 13.

Obviously, both the traditional IRIB-MDO and the proposed IRDB-MDO can obtain nearly the same optimal design of the supersonic aircraft conceptual design. However, as listed in Table 7, the number of total multidisciplinary analyses of

Table 7
Optimum solutions of IRIB-MDO and IRDB-MDO in case 3.

		IRIB-MDO[a]	IRDB-MDO[b]
Design variables	λ	0.113	0.100
	χ	1.036	1.170
	C_1	0.842	1.031
	T	0.248	0.248
	t/c	0.09	0.09
	h (ft)	60,000	60,000
	M	1.4	1.4
	AR	2.5	2.5
	Λ (°)	70	70
	S_{ref} (ft^2)	1500	1500
Reliability constraints	η_1	0.9	0.9
	η_2	1.0	1.0
Object	R	4248.7	4250.2
Total MDA	–	80,936	712

[a] ASA is utilized in IRIB-MDO.
[b] SQP is utilized in IRDB-MDO.

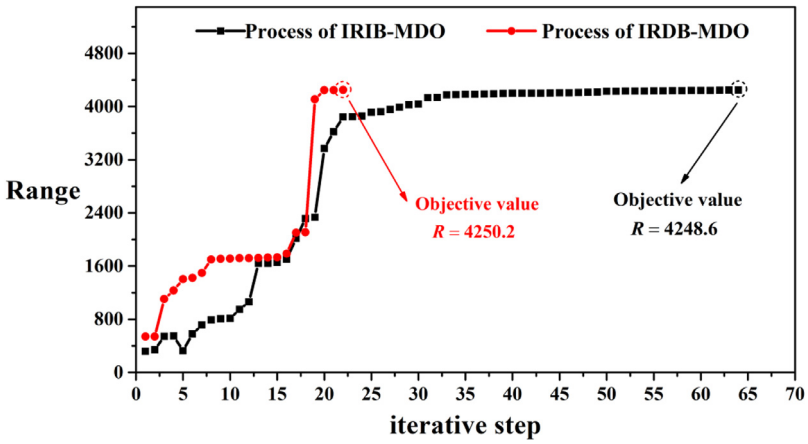

Fig. 13. Converging process of optimization based on IRIB-MDO and IRDB-MDO.

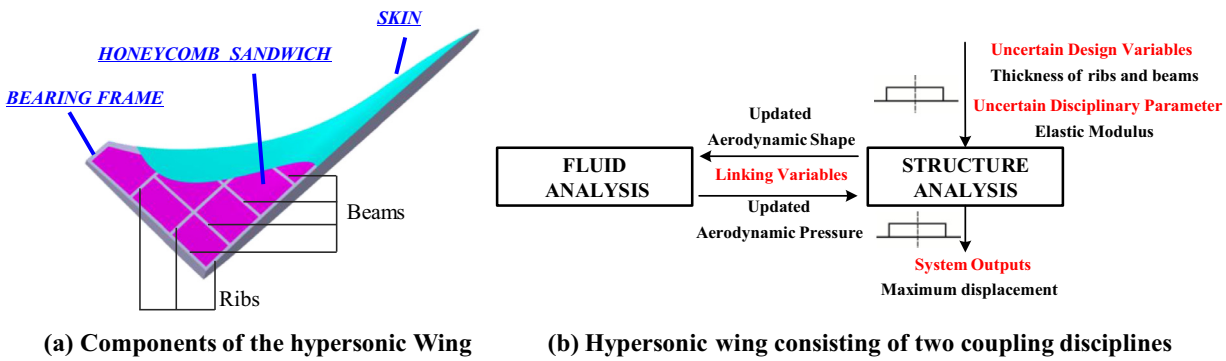

(a) Components of the hypersonic Wing **(b) Hypersonic wing consisting of two coupling disciplines**

Fig. 14. Illustration of the hypersonic wing design problem.

IRDB-MDO is 712 while that of IRIB-MDO is 80,936, which further verifies the high efficiency of IRDB-MDO for the high dimensional and highly non-linear multidisciplinary design problems.

5.3. Example 3: hypersonic wing design

The hypersonic wing design is selected as the engineering application for IRDB-MDO strategy in this example. As displayed in Fig. 14(a), the wing is composed of three part: (1) The titanium skin that covers the whole wing surface; (2) The bearing frame that consists of titanium alloy ribs and beams and (3) the sandwiches filled between ribs and beams with honeycomb paperboard. All the three components stick together to form the integrated wing structure.

Table 8
Uncertain descriptions of input variables in case 2.

	L_{rib}	L_{beam}	E_{Ti}	$d_{allowable}$
Median value	10 mm–50 mm	10 mm–50 mm	1.0e11 Pa	16 mm
Deviation	0.4 mm	0.4 mm	5.0e10 Pa	1.0 mm

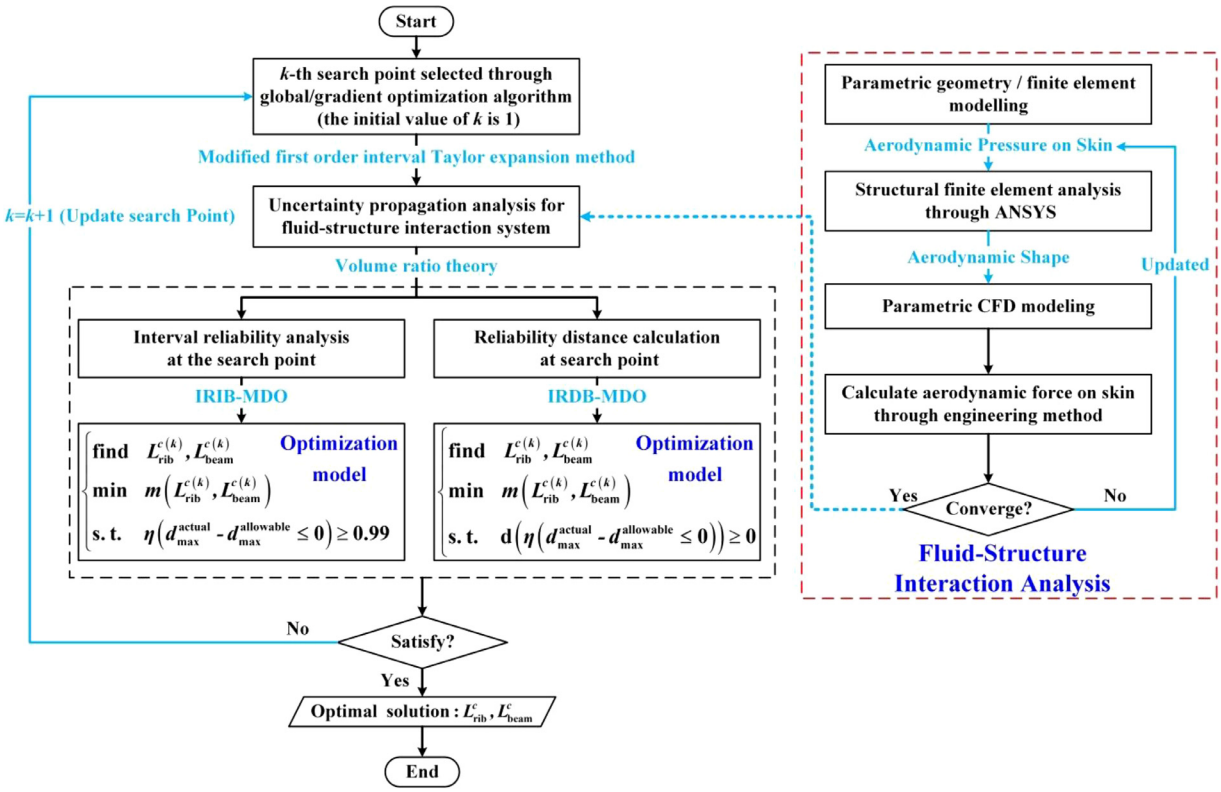

Fig. 15. Procedure of hypersonic wing design through IRIB-MDO and IRDB-MDO.

As shown in Fig. 14(b), the fluid discipline and structure discipline are strongly coupled in this case. And the design is formulated as UMDO problem to minimize the weight of the wing structure. Furthermore, the design variables include the thickness of the ribs L_{rib} and beams L_{beam}; the linking variables include the aerodynamic shape *Aero_shape* and pressure *Aero_pressure*; the output refers to the maximum displacement d_{max}^{actual}. Additionally, as described in Table 8, the elastic modulus of alloy materials E_{Ti}, the thickness of the ribs L_{rib} and beams L_{beam} as well as the allowable displacement $d_{allowable}$ are assumed to be uncertain due to the inevitable uncertainties in the process of design and manufacturing in practical engineering.

In this case, the reliability η_{dis} that the actual maximum displacement d_{max}^{actual} is less than the allowable displacement $d_{max}^{allowable}$ is taken as the constraint for the hypersonic wing design. The reliability can be mathematically expressed by

$$\eta_{dis} = \eta\left(d_{max}^{actual} \le d_{max}^{allowable}\right) \tag{35}$$

Of the two coupled disciplines, the aerodynamic pressure on the skin is computed by the engineering method and the structure analysis is conducted by finite element method. For flight environment, the flight altitude is 30 km, the free stream Mach number is 6 as well as the angle of attack is 16°. For the boundary conditions, the wing root region is imposed by fixed constraints to simulate the connection with the fuselage. The uncertainty propagation analysis for the fluid-structure interaction system is accomplished by the modified first order interval Taylor expansion method proposed in Section 2.2. Specially, the derivative in the global sensitivity equation is approximated by the finite difference method in this engineering case. And the procedure of the hypersonic wing design through both IRIB-MDO and IRDB-MDO is illustrated in Fig. 15.

As displayed in Fig. 16, in order to work out this engineering problem, the solution procedure is conducted by constructing the integrated optimization design platform with iSIGHT, which includes several modules: (1) CATIA that provides parametric modeling technology; (2) ANSYS that conducts finite element analysis; (3) MATLAB that calculates the interval reliability displacement and (4) the self-compiled program that obtains the aerodynamic pressure on the skin.

Table 9
Optimum solutions of IRIB-MDO and IRDB-MDO in case 3.

	Design variables		Object	Interval reliability		Total MDA
	L_{rib}	L_{beam}	m	η_1	η_2	
IRIB-MDO[a]	0.01	0.0175	524.4758	0.99110	0.99012	20,072
IRDB-MDO[b]	0.01	0.02143	524.3675	0.99004	0.99021	89

[a] ASA is utilized in IRIB-MDO.
[b] SQP is utilized in IRDB-MDO.

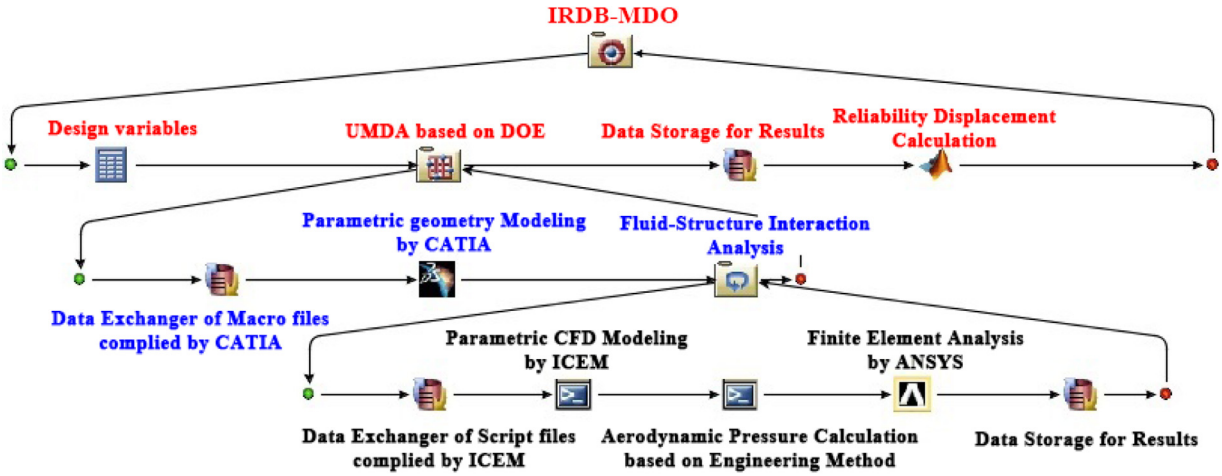

Fig. 16. Integrated platform for IRDB-MDO based on iSIGHT.

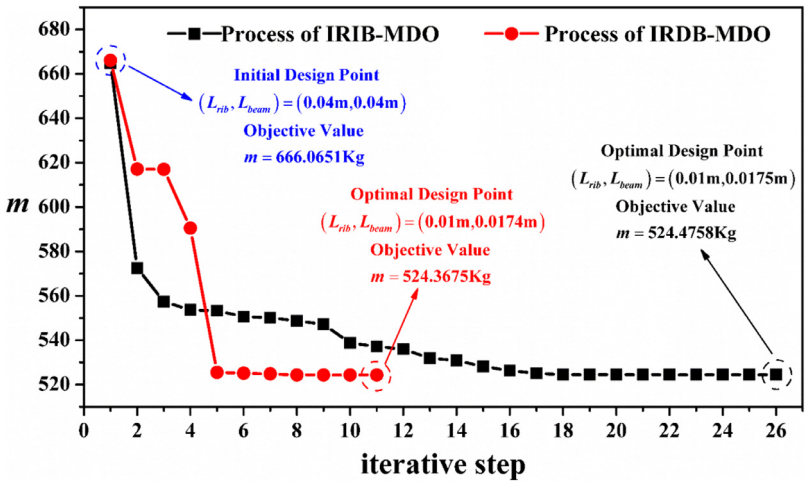

Fig. 17. Converging process of optimization based on IRIB-MDO and IRDB-MDO.

Based on the solving procedure in Fig. 16, the optimal design solutions can be listed in Table 9 and the converging processes of IRIB-MDO and IRDB-MDO are illustrated in Fig. 17. Moreover, the bounds of displacement at wing tip is illustrated in Fig. 18. Obviously, both strategies can obtain the optimal design of the hypersonic wing. Nevertheless, the number of total multidisciplinary analyses of IRDB-MDO is much less than IRIB-MDO since gradient optimum algorithm (SQP) is utilized in IRDB-MDO while global optimum algorithm (ASA) are utilized in IRIB-MDO, which indeed verifies the efficiency of the proposed IRDB-MDO.

5.4. Discussion

From the results of the three cases, the following conclusions can be summarized:

(1) As referred by the example 1, the traditional IRIB-MDO highly depends on the initial point when the gradient based methods are utilized. Once the initial point locates in the non-gradient region, the optimization process may be

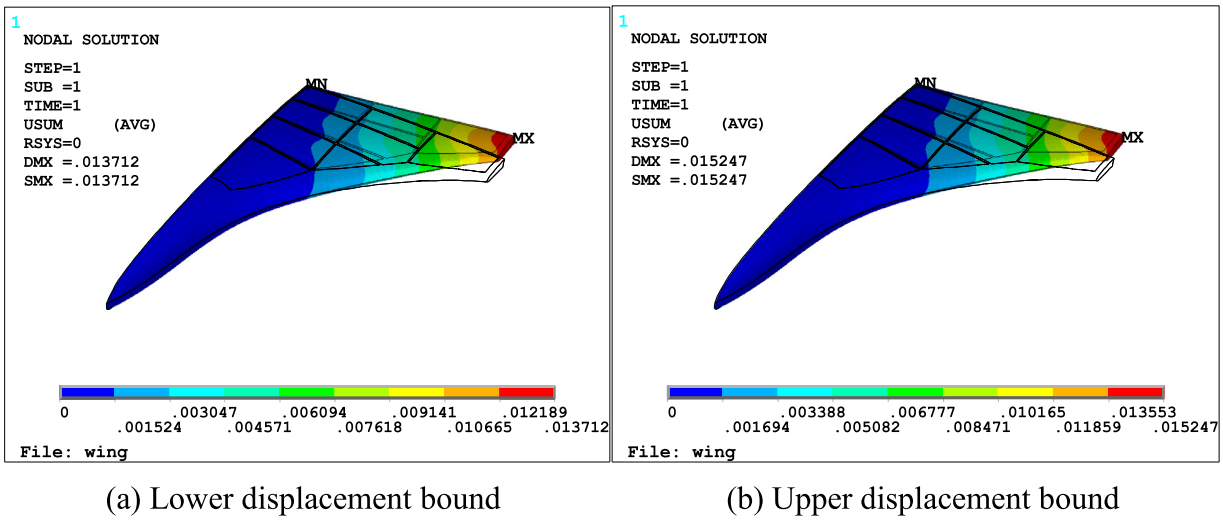

(a) Lower displacement bound (b) Upper displacement bound

Fig. 18. Bounds of displacement at wing tip for optimal design scheme.

delayed or misguided. Then the local optimal or the non-feasible solutions could be obtained. To overcome this, IRDB-MDO transforms all the design space into the gradient region through the equivalent transformation from the reliability index to the reliability displacement. Consequently, compared with IRIB-MDO, the optimization process based on IRDB-MDO could always be accelerated by utilizing gradient based optimization algorithms.

(2) As example 1 indicated, the probabilistic reliability for the design scheme obtained by either IRDB-MDO is larger than the interval reliability. Therefore, it is concluded that the design scheme based on either IRDB-MDO is more conservative than the ones based on probabilistic RBMDO for the reason that the available information in non-probabilistic RBMDO is less than that in probabilistic RBMDO.

(3) As example 2 and 3 stated, IRDB-MDO converges much faster than IRIB-MDO for that IRDB-MDO equivalently converts interval reliability into the displacement from the actual limit-state plane to the referential limit-state plane, and then the gradient information can be acquired under any circumstances. Consequently, the traditional gradient-based optimization algorithms can be utilized to acquire the global optimal solution, and then the convergence procedure is greatly accelerated. Thus, IRIB-MDO is indeed applicative in the optimization design of complicated engineering system.

6. Conclusions

Considering that the gradient information of the interval reliability cannot be fully obtained in the traditional NRBMDO problems, an interval reliability displacement based MDO method is proposed to promote the efficiency in this paper. The novel reliability displacement index is defined as the dynamic perpendicular displacement from the actual limit-state plane to the referential limit-state plane in IRDB-MDO. By replacing interval reliability with interval reliability displacement in the optimization model, the partial gradient domain is equivalently converted into whole gradient domain. IRDB-MDO possesses the following advantages over the traditional methods.

(1) Compared with the traditional IRIB-MDO strategy, the computational efficiency can be greatly promoted. For IRIB-MDO strategy, the time-consuming global optimization algorithms must be adopted to guarantee the global optimization solution due to the partial gradient domain. However, for IRDB-MDO strategy, the gradient optimization algorithms can be utilized because the whole gradient domain is obtained through the interval displacement index. And thus, the optimization process is sharply accelerated.

(2) Compared with the existing single loop strategy, IRDB-MDO is more robust. In the single level procedure, the outer optimization and inner reliability analysis are decoupled and executed in a sequential way to improve the computation efficiency. However, the iteration divergence may be caused in the highly non-linear problem due to the first-order approximation used in the constraint transformation. As for IRDB-MDO strategy, the original optimization framework is maintained and it is still a double-loop optimization problem in essence, thus the robustness can be ensured.

The proposed IRDB-MDO is tested with one numerical case and two complex practical engineering cases. The results show that it can obtain the optimum with lower computational cost than the traditional method, which demonstrates the effectiveness and efficiency of the proposed method. Moreover, to enhance the engineering applicability of IRDB-MDO, investigations are needed in the future to address the following issues: (1) novel reliability displacement index that involves

multi-source uncertainties and (2) the development of the more efficient strategy to deal with the RBMDO issue with large amount of design variables, uncertain parameters and constraints.

Acknowledgments

This work was supported by the National Natural Science Foundation of China (Grant Nos. 91016025, 11472276, 11332011); the Fundamental Research Funds for the Central Universities (No. ZY1814); and National Defense Basic Scientific Research program of China (No. JCKY2016130B009).

References

[1] J. Sobieszczanski-Sobieski, R. Haftka, Multidisciplinary aerospace design optimization: survey of recent developments, Struct. Multidiscip. Optim. 14 (1997) 1–23.
[2] J. Martins, A. Lambe, Multidisciplinary design optimization: a survey of architectures, AIAA J. 51 (2013) 2049–2075.
[3] T. Zang, M. Hemsch, M. Hilburger, S. Kenny, J. Luckring, P. Maghami, S. Padula, W. Stroud, Needs and Opportunities for Uncertainty-Based Multidisciplinary Design Methods for Aerospace Vehicles, Langley Research Center, 2002 NASA/TM-2002-211462.
[4] D. Padmanabhan, Reliability-based Optimization for Multidisciplinary System Design, University of Notre Dame, 2003.
[5] J. Roshanian, M. Ebrahimi, Latin hypercube sampling applied to reliability-based multidisciplinary design optimization of a launch vehicle, Aerosp. Sci. Technol. 8 (2013) 297–304.
[6] Y.S. Zhang, B. Zhao, Y.S. Liu, Z.F. Yue, Reliability-based multidisciplinary design optimization for centrifugal compressor using the fourth moment method, Adv. Mater. Res. 156-157 (2011) 575–581.
[7] D.B. Meng, Y.F. Li, H.Z. Huang, Z.L. Wang, Y. Liu, Reliability-based multidisciplinary design optimization using subset simulation analysis and its application in the hydraulic transmission mechanism design, J. Mech. Des. 137 (5) (2014) 051402.
[8] R.M. Paiva, C. Crawford, A. Suleman, Robust and reliability-based design optimization framework for wing design, AIAA J. 52 (2014) 711–724.
[9] H.U. Park, J. Chung, K. Behdinan, J.W. Lee, Multidisciplinary wing design optimization considering global sensitivity and uncertainty of approximation models, J. Mech. Sci. Technol. 28 (2014) 2231–2242.
[10] M. Nikbay, M.N. Kurut, Reliability based multidisciplinary optimization of aeroelastic systems with structural and aerodynamic uncertainties, J. Aircraft 50 (2013) 708–715.
[11] X.Q. Yu, X.P. Du, Reliability-based multidisciplinary optimization for aircraft wing design, Struct. Infrastruct. Eng. 2 (2006) 277–289.
[12] X. Yu, K.H. Chang, K.K. Choi, Probabilistic structural durability prediction, AIAA J. 36 (1998) 628–637.
[13] H.Z. Huang, H. Yu, X. Zhang, S. Zeng, Z. Wang, Collaborative optimization with inverse reliability for multidisciplinary systems uncertainty analysis, Eng. Optim. 42 (2010) 763–773.
[14] M. McDonald, S. Mahadevan, All-at-once multidisciplinary optimization with system and component-level reliability constraints, in: Proceedings of AIAA/ISSMO Multidisciplinary Analysis and Optimization Conference, 2008.
[15] Y. Ben-Haim, I. Elishakoff, Convex Models of Uncertainty in Applied Mechanics, Elsevier, Amsterdam, 1990.
[16] Y. Ben-Haim, A non-probabilistic concept of reliability, Struct. Saf. 14 (1994) 227–245.
[17] Y. Ben-Haim, A non-probabilistic measure of reliability of linear systems based on expansion of convex models, Struct. Saf. 17 (1995) 91–109.
[18] Y. Ben-Haim, I. Elishakoff, Discussion on: a non-probabilistic concept of reliability, Struct. Saf. 17 (3) (1995) 195–199.
[19] C. Jiang, R.G. Bi, G.Y. Lu, X. Han, Structural reliability analysis using non-probabilistic convex model, Comput. Method Appl. Mech. Eng. 254 (2013) 83–98.
[20] Z. Qiu, D. Yang, I. Elishakoff, Probabilistic interval reliability of structural systems, Int. J. Solids Struct. 5 (2008) 2850–2860.
[21] C. Jiang, X. Han, G.Y. Lu, J. Liu, Z. Zhang, Y.C. Ba, Correlation analysis of non-probabilistic convex model and corresponding structural reliability technique, Comput. Method Appl. Mech. Eng. 200 (2011) 2528–2546.
[22] Z.P. Qiu, J. Wang, The interval estimation of reliability for probabilistic and non-probabilistic hybrid structural system, Eng. Fail. Anal. 17 (2010) 1142–1154.
[23] L. Wang, X.J. Wang, R.X. Wang, X. Chen, Reliability-based design optimization under mixture of random, interval and convex uncertainties, Arch. Appl. Mech. 86 (2016) 1341–1367.
[24] Z. Kang, Y.J. Luo, Non-probabilistic reliability-based topology optimization of geometrically nonlinear structures using convex models, Comput. Methods Appl. Mech. Eng. 198 (2009) 3228–3238.
[25] S. Guo, Robust reliability method for non-fragile guaranteed cost control of parametric uncertain systems, Syst. Control Lett. 64 (2014) 27–35.
[26] S. Guo, Z. Lu, A non-probabilistic robust reliability method for analysis and design optimization of structures with uncertain-but-bounded parameters, Appl. Math. Model. 39 (2015) 1985–2002.
[27] Z. Kang, Y. Luo, A. Li, On non-probabilistic reliability-based design optimization of structures with uncertain-but-bounded parameters, Struct. Saf. 3 (2011) 196–205.
[28] C. Jiang, X. Han, G.R. Liu, Optimization of structures with uncertain constraints based on convex model and satisfaction degree of interval, Comput. Methods Appl. Mech. Eng. 196 (2007) 4791–4800.
[29] H. Ishibuchi, H. Tanaka, Multiobjective programming in optimization of the interval objective function, Eur. J. Oper. Res. 48 (1990) 219–225.
[30] X. Wang, Z. Qiu, I. Elishakoff, Non-probabilistic set-theoretic model for structural safety measure, Acta Mech. 198 (2008) 51–64.
[31] L. Wang, J.X. Liang, D. Wu, A non-probabilistic reliability-based topology optimization (NRBTO) method of continuum structures with convex uncertainties, Struct. Multidiscip. Optim. 58 (6) (2018) 2601–2620.
[32] X.Y. Geng, X.J. Wang, L. Wang, R.X. Wang, Non-probabilistic time-dependent kinematic reliability assessment for function generation mechanisms with joint clearances, Mech. Mach. Theory 104 (2016) 202–221.
[33] Y. Li, X. Wang, L. Wang, W.C. Fan, Z.P. Qiu, Non-probabilistic stability reliability measure for active vibration control system with interval parameters, J. Sound Vib. 387 (2017) 1–15.
[34] X. Wang, R. Wang, L. Wang, An efficient single-loop strategy for reliability-based multidisciplinary design optimization under non-probabilistic set theory, Aerosp. Sci. Technol. 73 (2018) 148–163.
[35] C. Jiang, X. Han, G.P. Liu, A sequential nonlinear interval number programming method for uncertain structures, Comput. Methods Appl. Mech. Eng. 197 (2008) 4250–4265.
[36] C. Jiang, X. Han, G.R. Liu, G.P. Liu, A nonlinear interval number programming method for uncertain optimization problems, Eur. J. Oper. Res. 188 (2008) 1–13.
[37] F.Y. Li, Z. Luo, G.Y. Sun, N. Zhang, An uncertain multidisciplinary design optimization method using interval convex models, Eng. Optim. 45 (2013) 697–718.
[38] X.J. Wang, R.X. Wang, X.J. Chen, X.Y. Geng, W.C. Fan, Interval prediction of responses for uncertain multidisciplinary system, Struct. Multidiscip. Optim. 55 (6) (2017) 1945–1964.
[39] Y.T. Zhou, C. Jiang, X. Han, Interval and subinterval analysis methods of the structural analysis and their error estimations, Int. J. Comput. Methods 3 (02) (2006) 229–244.

[40] Z. Qiu, I. Elishakoff, Antioptimization of structures with large uncertain but non random parameters via interval analysis, Comput. Methods Appl. Mech. Eng. 152 (1998) 361–372.
[41] C Fu, L Cao, J Tang, X Long, A subinterval decomposition analysis method for uncertain structures with large uncertainty parameters, Comput. Struct. 197 (2018) 58–69.
[42] J. Sobieszczanski-Sobieski, J. Agte, R. Sandusky, Bi-level integrated system synthesis (BLISS), in: Proceedings of the 7th AIAA/USAF/NASA/ISSMO symposium on multidisciplinary analysis and optimization, 2–4 September, St. Louis, MO, AIAA Press, NewYork, 1998 Article No. 98-4916.